



Title	Oceanic iron supply mechanisms which support the spring diatom bloom in the Oyashio region, western subarctic Pacific
Author(s)	Nishioka, Jun; Ono, Tsuneo; Saito, Hiroaki; Sakaoka, Keiichiro; Yoshimura, Takeshi
Citation	Journal of Geophysical Research, Oceans, 116, C02021 <a href="https://doi.org/10.1029/2010JC006321">https://doi.org/10.1029/2010JC006321</a>
Issue Date	2011-02-16
Doc URL	<a href="http://hdl.handle.net/2115/46928">http://hdl.handle.net/2115/46928</a>
Rights	Copyright 2011 by the American Geophysical Union.
Type	article
File Information	JGR116_C02021.pdf



[Instructions for use](#)

# Oceanic iron supply mechanisms which support the spring diatom bloom in the Oyashio region, western subarctic Pacific

Jun Nishioka,<sup>1</sup> Tsuneo Ono,<sup>2</sup> Hiroaki Saito,<sup>3</sup> Keiichiro Sakaoka,<sup>4</sup> and Takeshi Yoshimura<sup>5</sup>

Received 6 April 2010; revised 9 November 2010; accepted 7 December 2010; published 16 February 2011.

[1] Multiyear (2003–2008) time series observations along the A line provided information on the temporal variability of the dissolved iron (diss-Fe) concentration in the Oyashio region of the western subarctic Pacific, and the data indicated that there was an annual cycle in the concentration of surface diss-Fe occurring every year. Diss-Fe was supplied into the surface water in this region every winter and supports the spring phytoplankton bloom after development of the thermocline. The diss-Fe concentration was drawn down during the phytoplankton bloom period and was depleted in summer in some water masses. Then diss-Fe increased from autumn to winter with the increasing depth of the surface mixed layer. The high diss-Fe concentrations in the surface layer in winter were controlled by mesoscale oceanic intrinsic processes, such as vertical winter mixing and horizontal Fe-rich intermediate water transport. Difference in magnitude of the winter mixing processes among different water masses caused the heterogeneous distribution of diss-Fe concentration in the surface layer. Moreover, the vertical section profiles along a cross-Oyashio transect showed the occurrence of Fe-rich intermediate water, and upward transport of materials from the intermediate water to the surface layer via tidal and winter mixing processes are important mechanisms to explain the high winter surface diss-Fe concentrations. Additionally, the substantially higher diss-Fe/NO<sub>3</sub> ratio in the winter surface layer in this studied area other than the high-nutrient low-chlorophyll region indicates that the winter surface water in the Oyashio and the Oyashio-Kuroshio transition zone has a high potential to stimulate phytoplankton growth.

**Citation:** Nishioka, J., T. Ono, H. Saito, K. Sakaoka, and T. Yoshimura (2011), Oceanic iron supply mechanisms which support the spring diatom bloom in the Oyashio region, western subarctic Pacific, *J. Geophys. Res.*, 116, C02021, doi:10.1029/2010JC006321.

## 1. Introduction

[2] The western subarctic Pacific (WSP) is an area of confluence of water masses that are carried by the Oyashio, Kuroshio, and mesoscale eddies. The Oyashio is the western boundary current of the northern North Pacific, which is formed by cold, fresh, nutrient-rich upwelled waters from the western subarctic gyre flowing along the eastern side of the southern Kuril islands (Figure 1a). The Kuroshio, western boundary current of the subtropical North Pacific, transports warm, saline, nutrient-poor water into the mid-latitude of the North Pacific (Figure 1a). Previous studies have shown that the WSP has a larger seasonal amplitude in chlorophyll *a* and primary productivity than in the eastern subarctic Pacific (ESP) [Harrison *et al.*, 2004;

Chierici *et al.*, 2006]. Phytoplankton blooms regularly occur in spring in the Oyashio and Oyashio-Kuroshio transition zone [Saito *et al.*, 2002; Okamoto *et al.*, 2010], which corresponds with the area of the highest biological drawdown of *p*CO<sub>2</sub> and nutrient in the world ocean [Takahashi *et al.*, 2002; Chierici *et al.*, 2006]. Other previous studies showed that the WSP works as an effective biological pump and is an important region in the global carbon cycle [Longhurst *et al.*, 1995; Honda, 2003; Schlitzer, 2004; Buesseler *et al.*, 2007; Boyd *et al.*, 2008].

[3] On the other hand, despite the high biological productivity in the Oyashio and the Oyashio-Kuroshio transition zone, the whole subarctic Pacific is well known as one of the high-nutrient low-chlorophyll (HNLC) regions of the world's oceans and mesoscale iron (Fe) enrichment experiments conducted in subarctic Pacific clearly reveal that Fe limits phytoplankton growth [Tsuda *et al.*, 2003; Boyd *et al.*, 2004; Harrison *et al.*, 2004]. Since Fe is an essential micro-nutrient for the control of phytoplankton growth in the subarctic Pacific [Martin *et al.*, 1989], there is considerable interest in the seasonal cycle of the dissolved Fe (diss-Fe) concentration to determine the source and seasonal timing of input, which leads to the occurrence of the spring phyto-

<sup>1</sup>Pan-Okhotsk Research Center, Institute of Low Temperature Science, Hokkaido University, Sapporo, Japan.

<sup>2</sup>Hokkaido National Fisheries Research Institute, Kushiro, Japan.

<sup>3</sup>Tohoku National Fisheries Research Institute, Shiogama, Japan.

<sup>4</sup>Faculty of Fisheries Science, Hokkaido University, Hakodate, Japan.

<sup>5</sup>Central Research Institute of Electric Power Industry, Abiko, Japan.

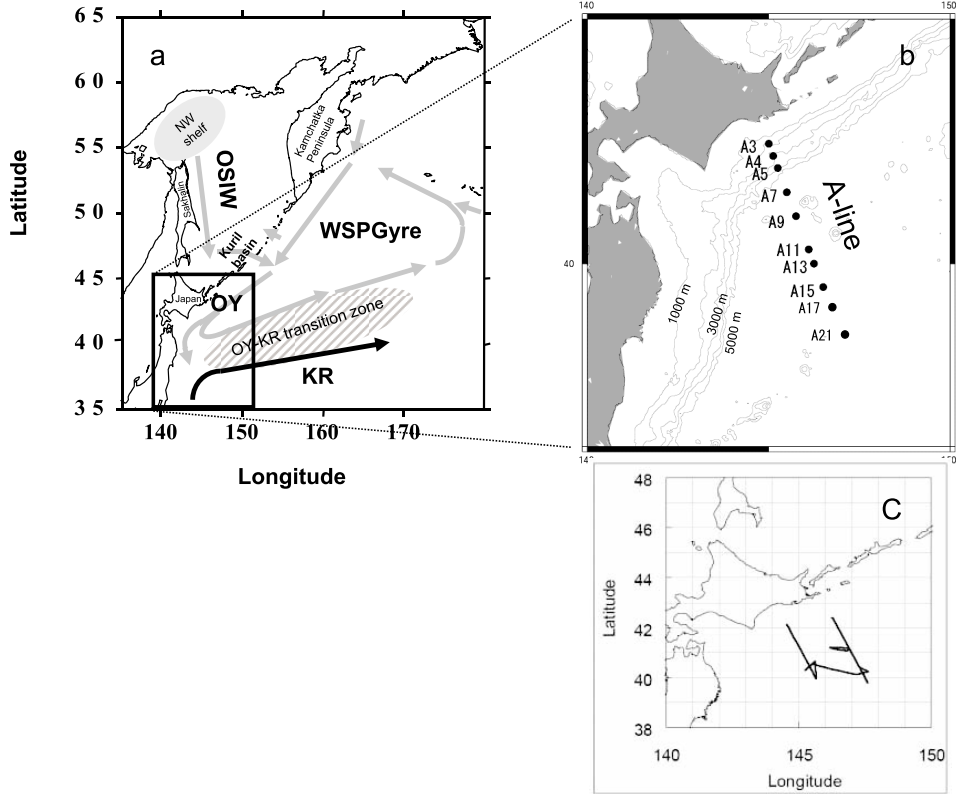


**Figure 1.** Schematic drawing of (a) the water structure in the western subarctic Pacific, (b) sampling stations along the observed A line and (c) ship's track of the underway survey in January 2008 of diss-Fe measurements in the Oyashio region. OY, Oyashio; KR, Kuroshio; OSIW, Okhotsk Sea Intermediate Water; WSP, western subarctic Pacific.

plankton bloom in the Oyashio and the Oyashio-Kuroshio transition zone.

[4] To date, atmospheric dust has been considered to be the most important source of Fe in this region. Previous studies indicate that there is a longitudinal dust gradient across the North Pacific, that is, the flux of dust containing Fe over the WSP is an order of magnitude higher than that in the ESP [e.g., *Duce and Tindale*, 1991; *Mahowald et al.*, 2005]. This is due to the close proximity to the second largest dust source in the world, the Gobi Desert, and this has been believed to be the leading cause for the longitudinal differences in biological production between the WSP and the ESP [*Harrison et al.*, 2004].

[5] On the other hand, recent studies have indicated that the source and the oceanic transport processes of Fe from the continental shelf are increasingly recognized as important for Fe supply to the open ocean [e.g., *Croot and Hunter*, 1998; *Elrod et al.*, 2004; *Johnson et al.*, 2005; *Moore and Braucher*, 2008]. In the Southern Ocean, another HNLC region, the potential contribution from multiple Fe sources including dust and oceanic Fe supply processes was evaluated quantitatively for regions adjacent to island or the Antarctic Peninsula [*Planquette et al.*, 2007; *Blain et al.*, 2008; *Dulaiova et al.*, 2009] and oceanic region [*Croot et al.*, 2004; *Ellwood et al.*, 2008; *Bowie et al.*, 2009]. As the Southern Ocean, oceanic Fe supply processes have reported in the subarctic Pacific [e.g., *Lam et al.*, 2006; *Nishioka et al.*, 2007; *Lam and Bishop*, 2008; *Cullen et al.*,

2009] in addition to atmospheric dust Fe supply. Therefore, we need more detailed investigations in order to clarify the dominant source of Fe which supports biological production in the subarctic Pacific.

[6] The temporal variability in the Fe concentration provides important information for determining Fe sources and has been studied in other regions of the coastal and open ocean surface of the North Pacific [e.g., *Johnson et al.*, 1999, 2001; *Elrod et al.*, 2008; *Boyle et al.*, 2005; *Chase et al.*, 2005]. The temporal variability of open ocean Fe concentrations in near surface waters in the central North Pacific indicated that the highest Fe concentrations were observed during periods of high Asian dust transport in spring and suggested the occurrence of significant interannual differences in the near surface Fe concentration responded to dust input [*Boyle et al.*, 2005]. In the ESP, vertical profiles of diss-Fe from the Ocean Station Papa (OSP) in different seasons showed little seasonal variation in the surface diss-Fe concentration, ranging between 0.06 and 0.10 nM with one exception in February 1999 (0.23 nM) [*Nishioka et al.*, 2001]. In the WSP, reported time series data, which only covered the winter to late spring season, showed a clear seasonal difference in the diss-Fe concentrations in the surface water [*Nishioka et al.*, 2007]. They also reported possible Fe supply processes into the WSP through intermediate water originating from the Sea of Okhotsk, in addition to the traditional view of dust Fe supply to this region [e.g., *Uematsu et al.*, 1983; *Duce and*

Tindale, 1991; Jickells and Spokes, 2001; Measures et al., 2005; Buck et al., 2006]. Additionally, lateral Fe transport from continental margin around Kamchatka [Lam and Bishop, 2008] is a possible source to the WSP. To date, however, time series data which cover all seasons have not been reported and the annual cycle in Fe concentrations has not been fully examined in the WSP.

[7] In this study, we report a long-term record of surface diss-Fe concentrations from 2003 to 2008 with a seasonal resolution along the monitoring observation line (A line) which crosses the Oyashio (Figure 1b) in order to detail the annual cycle of surface diss-Fe concentration. Additionally, underway surface Fe measurements along the ship's transect have been shown to be a good tool to collect Fe distribution data over a wide area in the surface layer [Vink and Measures, 2001; Johnson et al., 2003]. To elucidate the Fe supply process in this region, details of the spatial distribution of diss-Fe concentration in the winter surface (Figure 1c) were investigated by using underway autosequence sampling and analytical system, and also vertical sections of diss-Fe along the A line were measured. We then discuss the mechanism driving the annual cycle of surface diss-Fe concentration in this region.

## 2. Methods

### 2.1. Time Series Diss-Fe Observation

[8] The data presented here were obtained during one to eight cruises a year along the observation line of the Fisheries Research Agency (A line [Saito et al., 2002]) which crosses the Oyashio current (Figure 1b), from January 2003 to January 2008, using the R/V *Hokko-Maru*, *Wakataka-Maru*, *Tankai-Maru* and *Oshoro-Maru*. The data from January to May 2003 have previously been reported [Nishioka et al., 2007]. The cruise information in this study is shown in Table 1. From January 2003 until March 2004, samples were collected from the surface (10 m) to 800 m maximum at one to eight stations sampled regularly along the A line, using acid-cleaned Teflon coated 10 L X-Niskin sampling bottles suspended on a Kevlar line. From January 2005, acid-cleaned Teflon coated 10 L X-Niskin sampling bottles attached to a modified clean CTD-carousel multisampler system (CTD-CMS system: SBE-911 plus and SBE-32 water sampler Sea Bird Electronics Inc.), and samples were collected from 10 to 3000 m at six to nine stations along the A line. A comparison between sampling bottles on the Kevlar line and CTD-CMS was conducted during the January 2005 cruise, and no differences were observed between the sampling methods (Figure 2). The samples for diss-Fe measurement were filtered using 0.22  $\mu\text{m}$  acid-cleaned filters (Millipac-100, Millipore) under gravity pressure [Nishioka et al., 2007]. Details of the sampling are described by Nishioka et al. [2001, 2007]. All filtrate samples were adjusted to pH 3.2 with 10 M formic acid-2.4 M ammonium formate buffer solution and determined with an automatic Fe (III) flow injection analytical (FIA) system (Kimoto Electric, Ltd.) using chelating resin preconcentration and chemiluminescence detection [Obata et al., 1993]. These samples were allowed to sit at pH 3.2 for more than 1 day at room temperature and measured onboard or within onshore laboratory approximately 2 weeks after each cruise. We should note that to standardize the analysis methods through

the time series observation period, we acidified the all samples to pH 3.2 prior to analysis in this study. The determined diss-Fe concentration is in the form of chemically labile species which are leachable Fe in 0.22  $\mu\text{m}$  filtrate at pH 3.2 and strongly react with 8-hydroxyquinoline resin in the FIA chemiluminescence detection system [Obata et al., 1997]. All sample treatments were performed in a laminar flow clean air hood in the onboard laboratory.

[9] Our Fe measurement method and reference seawater were vetted by using SAFe cruise [Johnson et al. 2007] reference standard seawater (distributed by the Moss Landing Marine Laboratory (MLML) for an intercomparison study), with our results comparing favorably for dissolved iron concentration in  $\sim$ 0.1 and  $\sim$ 1 nM (SAFe reference standard seawater containing  $0.094 \pm 0.008$  nM (S) and  $0.923 \pm 0.029$  nM (D2) iron (<http://www.geotraces.org/>) were measured to be  $0.10 \pm 0.010$  nM ( $n = 3$ ) and  $0.99 \pm 0.023$  ( $n = 3$ ) by our method, respectively (the reference seawater was analyzed on 26 December 2006)).

[10] Nutrients and chlorophyll *a* concentrations were also analyzed for water samples. Nutrients concentrations were measured using a BRAN-LUEBBE autoanalyzer (TRACCS 800), and chlorophyll *a* concentrations were measured onboard by fluorometry (Turner Designs Model 10-AU) with nonacidified method as described by Welschmeyer [1994]. Hydrographic data was also collected at all stations using a CTD sensor. The surface mixed layer depth was calculated as the depth at which the potential density of the water column increased by 0.125 units [Levitus, 1982] relative to the sea surface.

### 2.2. Underway Diss-Fe Observations in the Winter Surface Layer

[11] In January 2008, clean surface water (1.5–4 m depth) was collected using a towed fish, metal-free sampling system [Tsumune et al., 2005]. The cruise track made a three-sided box around the A line and the ship's track during the underway observation is shown in Figure 1c. The system consists of 50 kg towed fish covered with metal-free epoxy paint and Teflon tubing (I.D. 12 mm) covered by PVC. The tubing was set through the center of the towed fish and the sample water flowed from the top of towed fish set on the side of the ship to the onboard laboratory, using an air-driven Teflon pump. The sample was filtered through a 0.22  $\mu\text{m}$  cartridge type filter (OPTICAP, Millipore) at the end of the tubing, and the sample led directly into an automatic Fe (III) flow injection analytical system (Kimoto Electric, Ltd.) which has an autosequence sampling system (J. Nishioka et al., manuscript in preparation, 2011). All sample treatments were conducted using an in-line system throughout sampling to analysis. This underway autosequence sampling and analytical system enables the measurement of diss-Fe concentrations in the surface layer with a high resolution (1 sample per 15–20 min) along the ship track with a 10–15 knot ship speed (diss-Fe was measured every 2.5–4 nautical miles). The determined diss-Fe concentration is in the form of chemically labile species which are in an immediately leachable form of Fe in 0.22  $\mu\text{m}$  filtrate at pH 3.2 and strongly react with 8-hydroxyquinoline resin in the FIA chemiluminescence detection system. Nitrate concentrations were also analyzed for water samples,

**Table 1.** Information on Time Series Iron Observation in the Oyashio Region Along the A Line<sup>a</sup>

Year	Month	Stations	Vessel	Cruise	Observed Minimum and Maximum Depth (m)		Sampling Method	Source
					Depth	Depth		
2003	Jan	A3, A4, A5, A7, A9, A11, A15	R/V <i>Hokko-Maru</i>	HK0301	10–800	Kevlar wire	reported by Nishioka et al. [2007]	
	Feb	A7	R/V <i>Oshoro-Maru</i>	OS131	10–300	Kevlar wire	reported by Nishioka et al. [2007]	
	Mar	A4, A7	R/V <i>Oshoro-Maru</i>	OS133	10–300	Kevlar wire	reported by Nishioka et al. [2007]	
	Apr	A4, A7, A11, A17	R/V <i>Wakataka-Maru</i>	WK0304	10–800	Kevlar wire	reported by Nishioka et al. [2007]	
	Apr (revisit)	A4, A7, A11	R/V <i>Wakataka-Maru</i>	WK0304	10–800	Kevlar wire	reported by Nishioka et al. [2007]	
	May	A4, A7, A11, A17	R/V <i>Wakataka-Maru</i>	WK0305	10–800	Kevlar wire	reported by Nishioka et al. [2007]	
	May (revisit)	A4, A7, A11	R/V <i>Wakataka-Maru</i>	WK0305	10–800	Kevlar wire	reported by Nishioka et al. [2007]	
	Oct	A3, A4, A5, A7, A9, A11, A13, A15	R/V <i>Hokko-Maru</i>	HK0310	10	Kevlar wire	reported by Nishioka et al. [2007]	
2004	Jan	A3, A4, A5, A7, A9, A11	R/V <i>Hokko-Maru</i>	HK0401	10–800	Kevlar wire	vertical section observation	
	Mar	A3, A4, A5, A7, A9, A11	R/V <i>Tankai-Maru</i>	TK0403	10	Kevlar wire	clean CTD-CMS system	
2005	Jan	A3, A4, A5, A7, A9, A11, A13, A15	R/V <i>Hokko-Maru</i>	HK0501	10–3000	clean CTD-CMS system	vertical section observation	
	Mar	A5, A7, A9, A11, A13, A17	R/V <i>Tankai-Maru</i>	TK0503	10	clean CTD-CMS system	clean CTD-CMS system	
	May	A3, A4, A5, A7, A9, A11, A13, A15, A17	R/V <i>Hokko-Maru</i>	HK0505	10–3000	clean CTD-CMS system	vertical section observation	
	July	A3, A4, A5, A7, A9, A11, A13, A15	R/V <i>Hokko-Maru</i>	HK0507	10	clean CTD-CMS system	clean CTD-CMS system	
	Sep	A3, A4, A5, A7, A9, A11, A13, A15, A17	R/V <i>Hokko-Maru</i>	HK0509	10	clean CTD-CMS system	vertical section observation	
	Dec	A4, A5, A7, A9, A11, A13, A15, A17	R/V <i>Hokko-Maru</i>	HK0512	10–3000	clean CTD-CMS system	clean CTD-CMS system	
2006	Jan	A4, A5, A7, A9, A11, A13, A15, A17	R/V <i>Hokko-Maru</i>	HK0601	10–3000	clean CTD-CMS system	vertical section observation	
	Jan	A3, A4, A5, A7, A9, A11, A13, A15, A17	R/V <i>Hokko-Maru</i>	HK0701	10	clean CTD-CMS system	vertical section observation	
2007	May	A3, A4, A5, A7, A9, A11, A13	R/V <i>Hokko-Maru</i>	HK0705	10	clean CTD-CMS system	vertical section observation	
	Oct	A3, A4, A5, A7, A9, A11, A13, A15, A17	R/V <i>Hokko-Maru</i>	HK0710	10	clean CTD-CMS system	vertical section observation	
2008	Jan	A4, A5, A7, A9, A11, A13, A15, A17	R/V <i>Hokko-Maru</i>	HK0801	10	clean CTD-CMS system	underway observation	

<sup>a</sup>Year, date, stations, vessel, cruise, observed depth range, and sampling method.

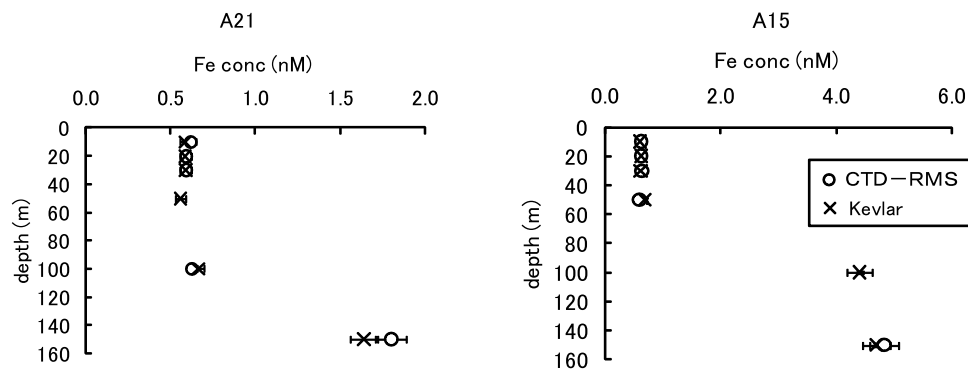


**Figure 2.** Results of the comparison between sampler bottles on the Kevlar line and CTD-CMS conducted during the January 2005 cruise. Error bars represent relative standard deviation within 5% for replicate measurements of a standard seawater sample during test cruise, some are smaller than symbols.

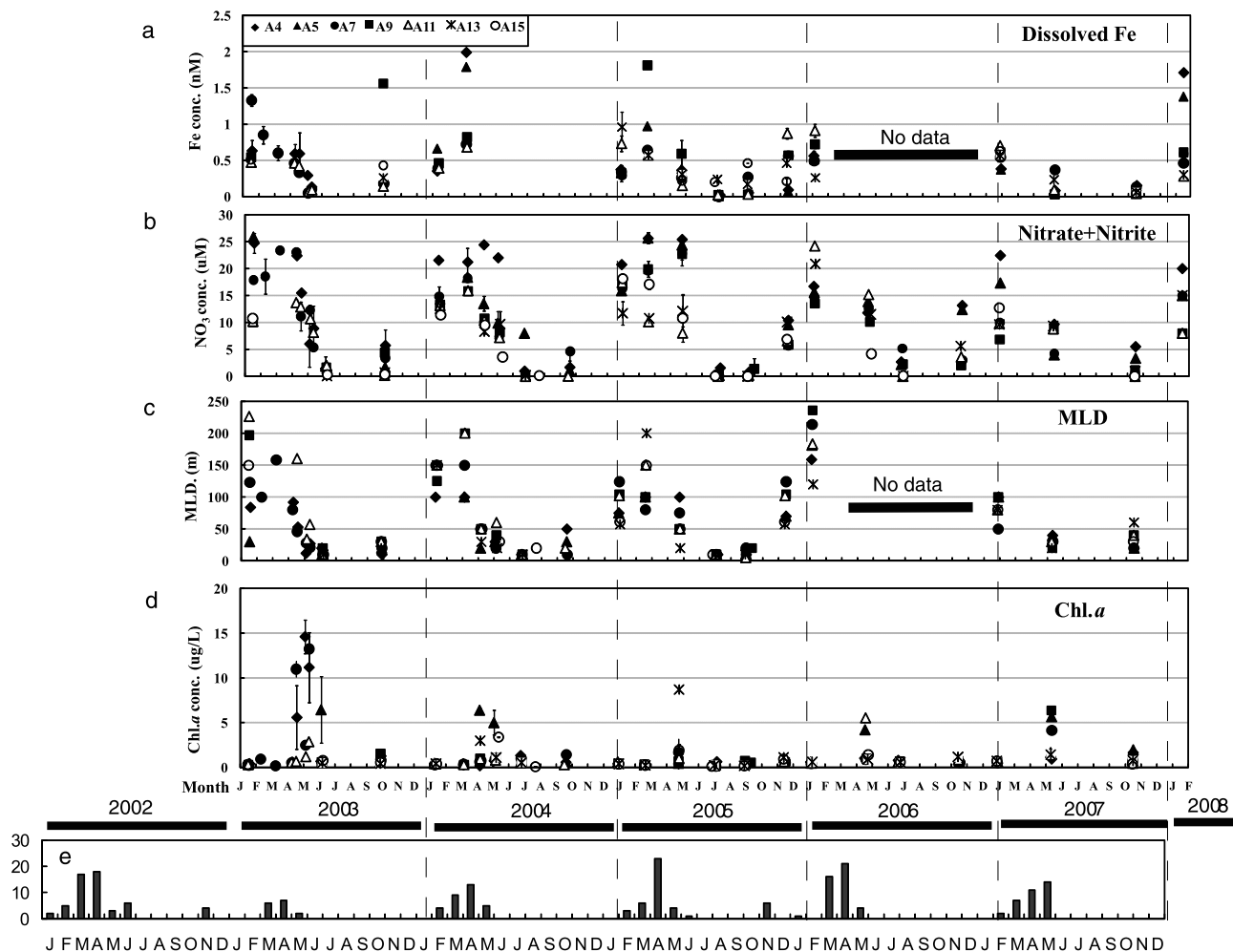


**Figure 3.** Changes in (a) surface diss-Fe concentrations, (b) surface nitrate concentrations, (c) surface mixed layer depth (MLD), (d) surface chlorophyll *a* concentrations, and (e) number of the dust events which were observed by the Japan Meteorological Agency at 69 meteorological stations throughout Japan using visually transmittance survey ([http://www.data.kishou.go.jp/obs-env/kosahp/kosa\\_table\\_1.html](http://www.data.kishou.go.jp/obs-env/kosahp/kosa_table_1.html)) from January 2003 to January 2008.

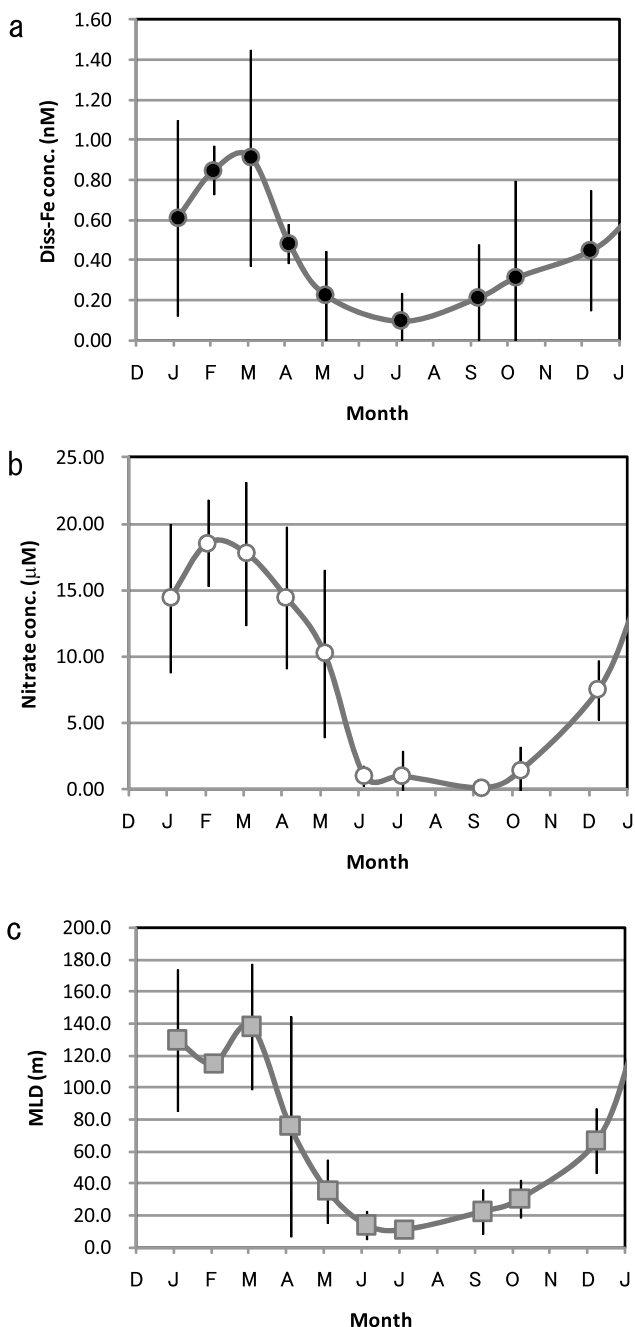


**Figure 4.** Monthly compiled (a) surface diss-Fe concentration, (b) nitrate concentration, and (c) mixed layer depth along the A line in the Oyashio region. (For Figures 4a and 4b, the plots are the mean values of all concentrations in the surface mixed layer in each month which are presented in Table S1.) Error bars represent  $\pm 1\text{SD}$  value.

which were collected from the end of sampling tubing every 15–30 min.

### 3. Results

#### 3.1. Time Series Data of Surface Diss-Fe Concentrations

[12] Diss-Fe concentrations along A line were measured, and changes in surface (mean value of concentrations in the

surface mixed layer or concentrations at 10 m depth) diss-Fe concentrations, surface nitrate concentrations, surface mixed layer depth (MLD), surface chlorophyll *a* concentrations, from January 2003 to January 2008 are shown in Figure 3 and Table S1 in the auxiliary material.<sup>1</sup>

[13] Mineral aerosols from the Asian continent are transported to the North Pacific. High mineral dust concentrations have been frequently observed in spring and transported by the movement of a low-pressure system over Japan [Uematsu *et al.*, 2002]. The number of dust events observed by the Japan Meteorological Agency at 69 meteorological stations throughout Japan using a visual transmittance survey ([http://www.data.kishou.go.jp/obs-env/kosahp/kosa\\_table\\_1.html](http://www.data.kishou.go.jp/obs-env/kosahp/kosa_table_1.html)) is shown in Figure 3e.

[14] Mean monthly compiled data (from the same data set as Figure 3 and Table S1) for the 5 year studied period of the surface diss-Fe and nitrate concentrations, and MLD along A line are shown in Figure 4. In the coastal area of this region, there is the Coastal Oyashio water which has different characteristics (identified by surface salinity <33.0 [Ohtani, 1989]; see section 3.2). The processes which control seasonality of Fe concentrations in the Coastal Oyashio water are probably different from the Oyashio and Oyashio-Kuroshio transition zone. Therefore, to avoid influence of the Coastal Oyashio water, the plotted data in the Figures 3 and 4 were selected from A4 to A15 (these stations include the Oyashio water and part of the Oyashio-Kuroshio transition zone), except A4 May 2005 which data was excluded due to clearly influence of surface flow of the coastal water.

[15] This time series observations show an annual cycle of the diss-Fe concentration in the surface layer in this studied area as follows.

[16] 1. In “winter,” from the monthly compiled data, maximum value ( $0.92 \pm 0.54 \text{ nM}$ , mean  $\pm 1\text{SD}$ , monthly compiled data in Figure 4a) is recorded in March when the surface mixed layer became deepest, the same as nitrate (Figure 4b).

[17] 2. In “spring,” a shallow thermocline was formed in the surface layer (Figure 4c) and both of the diss-Fe and nitrate concentration decreased during the spring phytoplankton bloom (Figures 3a, 3b, 3d, 4a, and 4b). It is also noteworthy that we observed some depleted values of diss-Fe concentrations at some stations along the A line in May (Figures 3a and 4a and Table S1), when high nitrate concentrations ( $10.25 \pm 6.28 \mu\text{M}$ ) still remain in the surface water (Figure 4b and Table S1).

[18] 3. In “summer,” diss-Fe was depleted in summer in some stations ( $0.10 \pm 0.14 \text{ nM}$ , mean  $\pm 1\text{SD}$ , monthly compiled data in July in Figure 4a) along the observed line.

[19] 4. In “autumn to winter,” diss-Fe concentration increased from autumn to winter ( $0.61 \pm 0.49 \text{ nM}$ , mean  $\pm 1\text{SD}$ , monthly compiled data in January in Figure 4a) with the increase of MLD (Figure 4c).

#### 3.2. Spatial Distribution of Diss-Fe in the Winter Surface Layer

[20] The results of surface salinity, temperature, diss-Fe concentration and nitrate concentration measurements using the underway autosequence sampling analytical system

<sup>1</sup>Auxiliary materials are available in the HTML. doi:10.1029/2010JC006321.

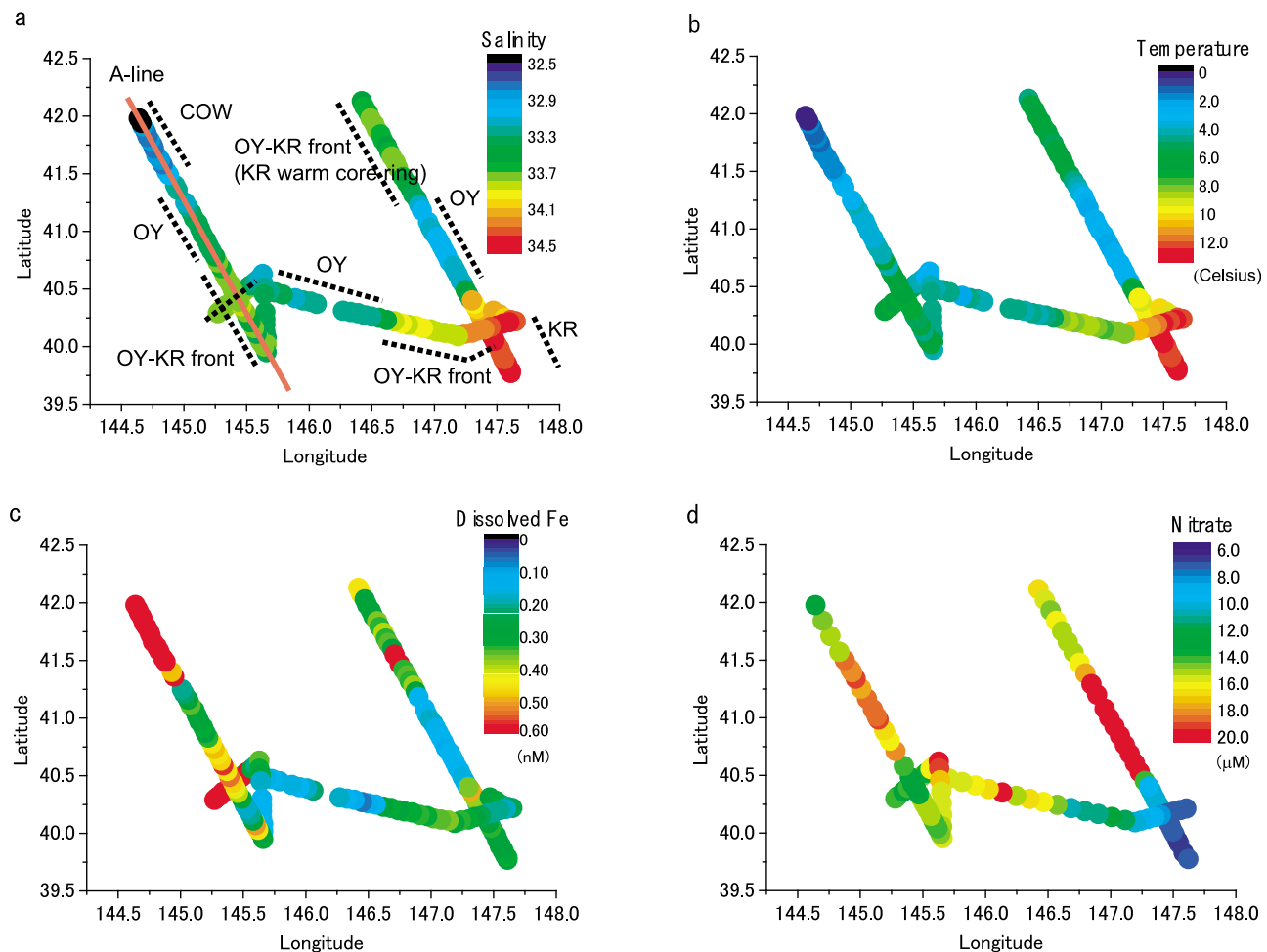


**Figure 5.** Surface counter plot of (a) sea surface salinity, (b) temperature, (c) surface diss-Fe concentrations, and (d) nitrate concentrations during underway observations in January 2008 in the Oyashio region. COW, Coastal Oyashio water; OY, Oyashio; KR, Kuroshio.

conducted in winter, January 2008, are shown in Figure 5 and Table S2. The diss-Fe concentration level in the surface layer clearly changed with the changing mesoscale water hydrographic features, such as the water properties of salinity and temperature (Figures 5a, 5b, and 5c). The area we observed was occupied by Coastal Oyashio water (surface salinity <33.0 [Ohtani, 1989]), Oyashio water (surface salinity 33.0–33.6 [Ono et al., 2005]), Kuroshio-oriented warm water (salinity >34.0 [Ono et al., 2005]), and the front water between Oyashio water and Kuroshio-oriented warm water (surface salinity 33.6–34.0). Among these, the Coastal Oyashio water has the highest diss-Fe concentration up to 2.8 nM (Figure 5c). Although the other waters had moderately high diss-Fe concentrations (mean  $0.33 \pm 0.18$  nM; mean  $\pm 1$  SD, Figure 5c), our data showed that the center of both Oyashio water domain and Kuroshio-oriented warm water domain has relatively low diss-Fe value ( $\sim 0.2$  nM). The front water generally showed relatively high diss-Fe values (0.3–0.6 nM).

### 3.3. Vertical Section Fe Distribution Along A Line

[21] Section profiles of temperature and salinity along the A line in January and December 2005 and January 2006 are shown in Figure 6. The section profiles of diss-Fe con-

centrations are shown in Figure 7. All data are shown in Table S3. The section for diss-Fe indicates that the diss-Fe concentrations in winter were substantial in the surface mixed layer ( $0.53 \pm 0.25$  nM, mean  $\pm 1$  SD, mean value of all data from MLD in January 2005, December 2005, January 2006), and higher in the intermediate water ( $1.36 \pm 0.50$  nM, mean  $\pm 1$  SD, mean value of all data in intermediate water ( $26.6\text{--}27.5 \sigma_0$ ) in January and December 2005 and January 2006). The core of high diss-Fe concentrations of the intermediate water is consistent with Okhotsk Sea Intermediate Water (OSIW) [Yasuda et al., 2001; Ohshima et al., 2010], which contain high concentration of Fe [Nishioka et al., 2007].

## 4. Discussion

### 4.1. Annual Cycle of Diss-Fe Concentration

[22] Nishioka et al. [2007] reported the seasonal variation of surface diss-Fe, nitrate, MLD and chlorophyll *a* concentration from January to May 2003, and the pattern of seasonal change in diss-Fe concentration in the surface mixed layer was similar to that of macronutrients. These results suggested that deep winter water mixing resulted in relatively high winter concentration of Fe in the surface

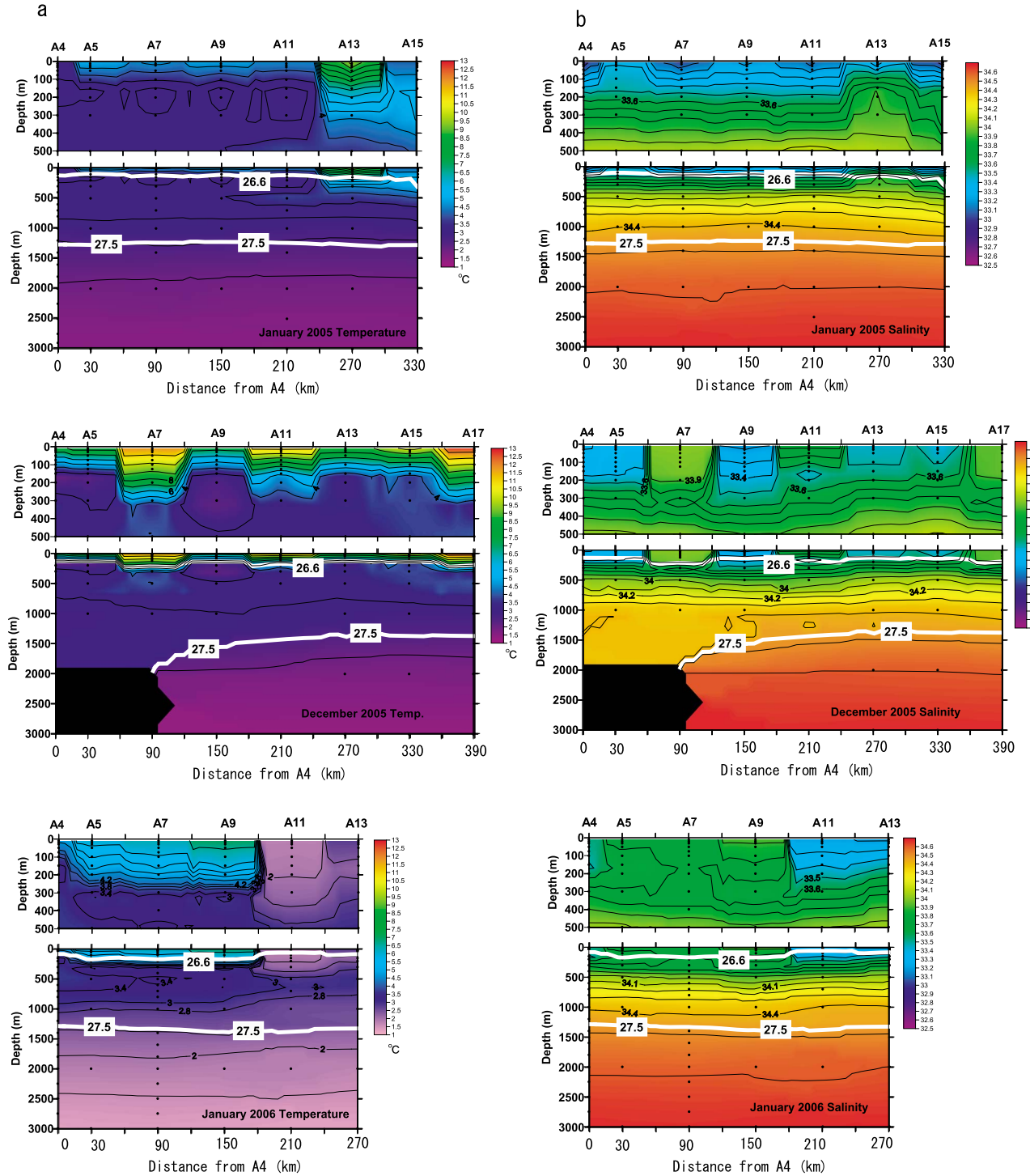


**Figure 6.** Vertical section profiles of (a) temperature and (b) salinity along the A line in January 2005, December 2005, and January 2006.

water of this region. The longer-term time series observations in this study clearly show an annual cycle of the diss-Fe concentration in the surface layer in this studied area, which occurred every year (Figures 3a and 4a). High diss-Fe levels in the surface mixed layer were detected every winter from 2003 to 2008, implying that Fe is supplied every winter into the surface water (Figure 3a).

[23] To discuss the Fe supply processes which drive the annual cycle of the surface diss-Fe concentration, the time series diss-Fe concentration were plotted with the monthly variation in the number of dust events in Figures 3a and 3e. Dust events were rare in autumn to winter, and this is the period during which the surface diss-Fe concentration increased. Therefore, although a part of the surface diss-Fe concentrations may be affected by the spring dust Fe supply,

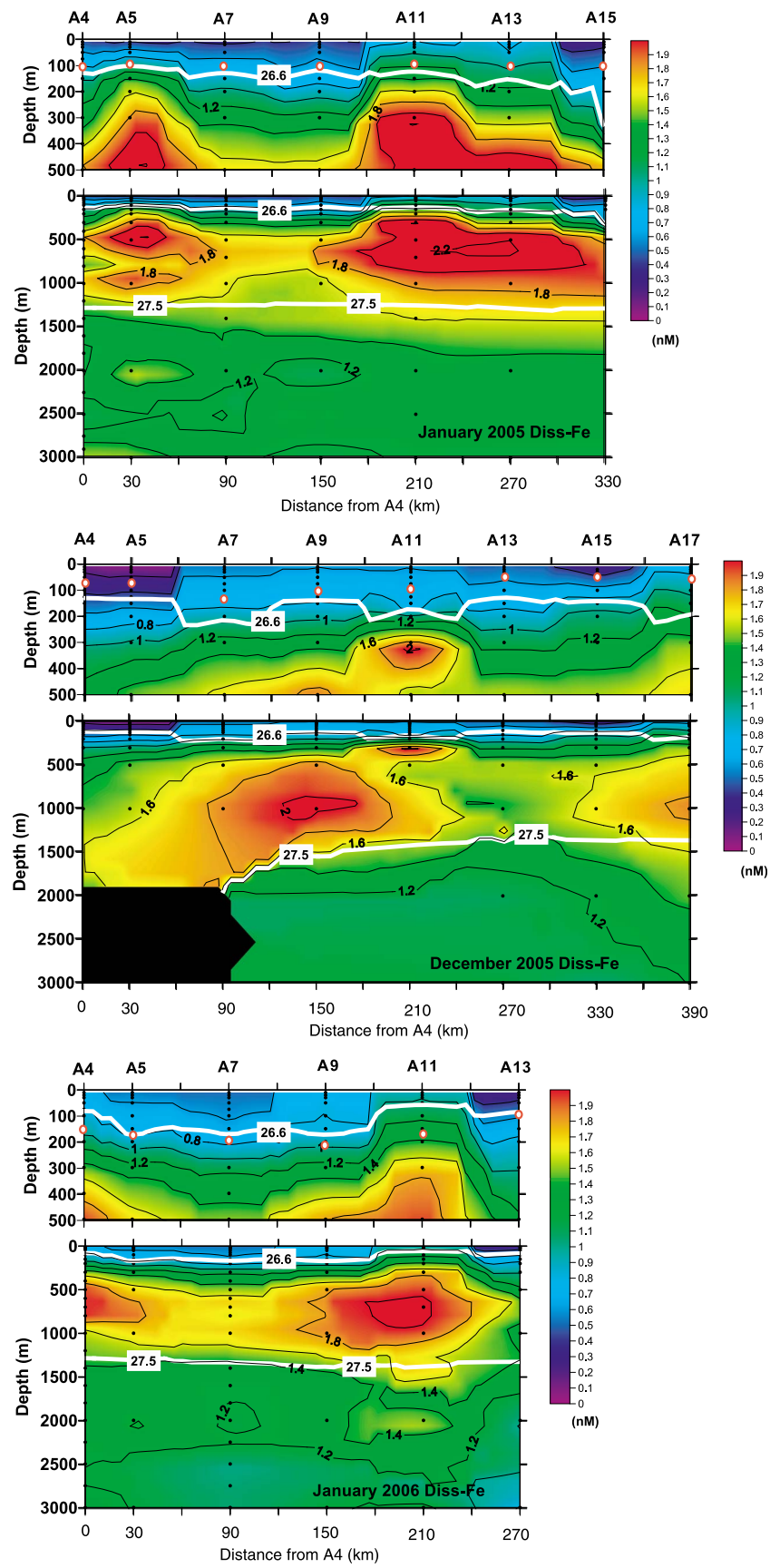


**Figure 7.** Vertical section profiles of diss-Fe along the A line in January 2005, December 2005, and January 2006. Red dots in Figure 7 (top) indicate observed surface mixed layer depth.

dust events probably do not markedly contribute to the high diss-Fe concentration in the winter surface mixed layer and the annual cycle of the surface diss-Fe in the Oyashio and Oyashio-Kuroshio transition zone.

[24] The diss-Fe concentrations decreased every spring with the increase in chlorophyll *a* concentrations, and was depleted in some stations in summer (Figures 3a and 4a and Table S1). Part of this is probably due to the biological uptake of diss-Fe during the spring phytoplankton bloom. The previously conducted mesoscale Fe enrichment experiment in the subarctic North Pacific clearly showed that artificially enriched Fe in the dissolved fraction was rapidly transformed into suspended labile particulate Fe during phytoplankton growth due to aggregate to particles and reduced Fe bioavailability [Nishioka et al., 2003]. Therefore, in addition to the biological uptake, the transformation process probably occurs also during the natural spring phytoplankton bloom. The transformation process reduces the diss-Fe concentration and its bioavailability, and may affect the termination of the bloom.

#### 4.2. Diss-Fe Supply in the Winter Surface Layer

[25] We discuss here the potential sources of Fe which can explain the high diss-Fe levels in the surface mixed layer in winter. Details of the spatial distribution of diss-Fe with water mass hydrographic features in the surface are important for understanding the Fe supply processes to the ocean surface. The spatial scale of atmospheric dust events is well larger than that of oceanic intrinsic physical processes, such as eddy, jet and turbulent upwelling processes. Therefore, if atmospheric Fe input dominates the Fe supply to the surface layer, the diss-Fe concentration would not vary with water mass hydrographic features. While, if diss-Fe concentrations vary with the water mass hydrographic features, the concentrations can be considered to be controlled by oceanic processes, such as winter turbulence, vertical mixing and upwelling/downwelling of each water mass.

[26] The heterogeneity of the spatial distribution of diss-Fe concentrations explains the wide range of surface water values found throughout the course of the time series study and clearly depicts an association with various water masses. The diss-Fe concentration level in the surface layer in January 2008 clearly changed with the changing mesoscale water hydrographic features, such as the thermohaline properties (Figures 5a, 5b, and 5c), and the Oyashio front water generally showed relatively high diss-Fe values. The diss-Fe varied with the mesoscale water mass hydrographic features (Figure 5c), indicating that diss-Fe concentrations in the winter surface layer in the Oyashio and Oyashio-Kuroshio transition zone were controlled by oceanic processes, such as vertical mixing.

[27] In winter, it is known that strong vertical water exchange occurs rather in the Oyashio front area than in the center of the Oyashio domain [Talley, 1991; Suga et al., 2004; T. Nakamura et al., manuscript in preparation, 2011]. This process well explains the observed 2-D surface diss-Fe distribution (Figure 5c), with the assumption that the high diss-Fe water in the winter surface was supplied from below the surface through winter vertical water mixing. Conversely, strong vertical mixing in the Oyashio front area should lead to lower diss-Fe concentration than in the Oyashio domain waters, if we assume airborne dust as the

main Fe source. It is concluded that the winter mixing process is one of the important factors for explaining the high level of diss-Fe concentration and its heterogeneous distribution in the surface Oyashio and Oyashio-Kuroshio transition zone in winter.

#### 4.3. Diss-Fe in the Intermediate Water: The Fe Source Water

[28] It has been reported that the Oyashio region waters originate partly from the Sea of Okhotsk water with a density range 26.6–27.5  $\sigma_0$  [Yasuda et al., 2001; Ohshima et al., 2010]. Additionally, our previous study indicated that water ventilation processes in this region [Talley, 1991; Yasuda, 1997], which are driven by the sea ice formation, control the transport of sedimentary Fe through the intermediate water layer from the northwestern continental shelf of the Sea of Okhotsk to a wide area of the WSP [Nishioka et al., 2007]. The vertical profiles of diss-Fe in the Oyashio region are a result of the remineralization of particulate Fe which was vertically transported and laterally transported diss-Fe. We use  $Fe^*$  to evaluate the contribution of the laterally transported diss-Fe in this section profile. The  $Fe^*$  is modified from Parekh et al. [2005] as

$$Fe^* = [diss - Fe]_{(observed)} - [PO_4]_{(observed)} \times R_{Fe:P}$$

where  $[diss-Fe]$  and  $[PO_4]$  are the observed concentration values in this study and  $R_{Fe:P}$  represent the ratio of diss-Fe to  $PO_4$ , the value is 0.47, the same ratio as in the work by Parekh et al. [2005] (assuming a fixed Fe:C ratio of 4 mmol:1 mol and a C:P Redfield ratio of 117:1 [Anderson and Sarmiento, 1994]).  $Fe^*$  is defined as the Fe supplied from an external source decoupled from the phosphate (regeneration) cycle. In this study, therefore, laterally transported diss-Fe is defined as the  $Fe^*$  value and remineralized diss-Fe is defined as the equation of “[Diss-Fe] –  $[Fe^*]$ .” The calculated laterally transported diss-Fe is probably underestimated because we did not account for Fe scavenging processes and preformed  $PO_4$  in “[ $PO_4$ ]<sub>(observed)</sub> ×  $R_{Fe:P}$ .<sub>”</sub> A vertical profile of diss-Fe concentration, laterally transported diss-Fe and remineralized diss-Fe at station A11 in the January 2005 is shown in Figure 8. Vertical section profiles of  $Fe^*$  value along the A line in January 2005, December 2005, and January 2006 are shown in Figure 9a. The core of the diss-Fe rich intermediate water in the Oyashio region is consistent with the density range in 26.6–27.5  $\sigma_0$  (Figures 7, 8, and 9a), and  $Fe^*$  value is also especially high in the density range (Figures 8 and 9a). Estimation form the  $Fe^*$  value indicate that 30–50% of diss-Fe in the Fe-rich intermediate water was added by lateral advection at upstream of the Oyashio current. These results are compatible with previous reported data that the Fe-rich intermediate water is transported from the Sea of Okhotsk to WSP [Nishioka et al., 2007], and laterally Fe transport from continental margin around Kamchatka [Lam and Bishop, 2008]. We can estimate the amount of diss-Fe which is laterally transported by the intermediate Oyashio water. Geostrophic transport of Oyashio components in the intermediate layer (26.6–27.2  $\sigma_0$ ) was estimated to 5–6 Sv ( $10^6 m^3 s^{-1}$ ) [Shimizu et al., 2003]. If we employed the mean value of diss-Fe concentration (1.36 nM) in the intermediate water, 30%–50% portion of lateral transported diss-Fe calculated

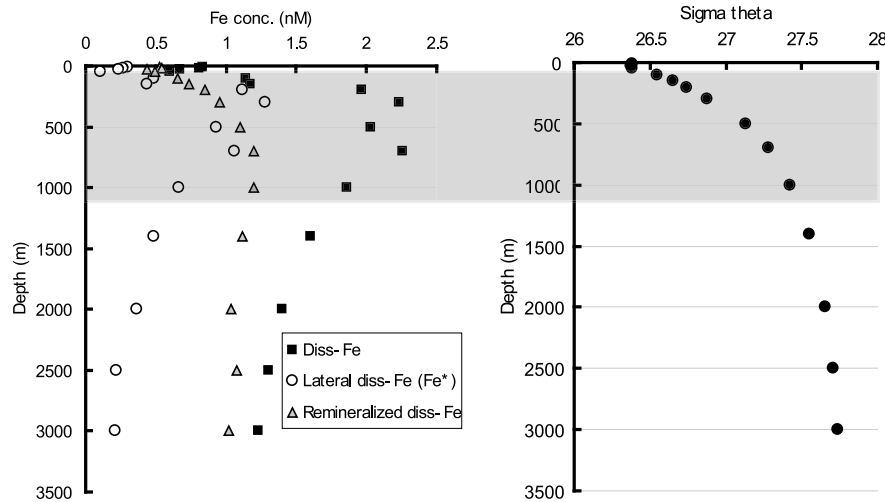


**Figure 8.** (left) Vertical profiles of diss-Fe concentration, laterally transported diss-Fe and remineralized diss-Fe at station A11 in the January 2005. The laterally transported diss-Fe is defined as  $[\text{Fe}^*]$  value and the remineralized diss-Fe is defined as equation of “[Diss-Fe] –  $[\text{Fe}^*]$ .” (right) Vertical profile of density value ( $\sigma_\theta$ ) is plotted. Density range between 26.6 and  $27.5\sigma_\theta$  is hatched.

from  $\text{Fe}^*$  and the reported geostrophic transport of the intermediate water Oyashio components, the amount of diss-Fe which is laterally transported to the intermediate Oyashio water is  $5.3 \times 10^6$  to  $10.6 \times 10^6 \text{ mol month}^{-1}$ . If we employ a flux estimation for cross the A line (A4 to A15: 330 km) intermediate layer section (for this calculation, 850 m) and assume that there is no seasonal variation, the lateral transport flux of diss-Fe in the intermediate layer section along A line is  $2.3 \times 10^5$  to  $4.5 \times 10^5 \mu\text{mol Fe m}^{-2} \text{ yr}^{-1}$ . This value is enormous relative to upward diss-Fe flux which described in section 4.4.

[29] Maximum winter mixed layer occur in March, but we could not conduct detailed section observation in March because of logistics reason. However, a previous study provides evidence that the winter MLD reaches the depth of the Fe-rich intermediate water. *Talley* [1991] reported water maximum sea surface density in the WSP, based on all available observation data. This study clearly indicated that dense water (which has density range in  $26.6\text{--}26.7 \sigma_\theta$ ) appears in winter surface in the southwestern corner of the subpolar western subarctic gyre, the Oyashio and Oyashio-Kuroshio transition zone, results from mixing of cold, fresh waters from the Oyashio with saltier waters from the Kuroshio together with winter cooling. One of our data in January 2006 clearly indicate that surface winter MLD reached to the core of the Fe-rich intermediate water depth ( $26.6 \sigma_\theta$ ) directly (Figure 7), though the observation was before March. Our data also showed that the mechanism bringing diss-Fe from the Fe-rich intermediate water to winter surface layer cannot be solely explained by the deep winter mixing, because surface diss-Fe concentration was enriched in nanomolar to subnanomolar level even though winter MLD did not reach to the depth of the core of the Fe-rich intermediate water ( $26.6 \sigma_\theta$ ) in January 2005 and December 2005 (Figure 7). Mixing induced by the motion of an eddy is one of important process to bridge this depth gap. Additionally, another substantial mechanism bridging

the depth gap exists in this region. In 2006 summer, the investigations of Fe concentrations with physical parameters at the Kuril straits have conducted to study tidally generated internal waves influence to the Fe-rich OSIW. The observation clearly revealed that the Fe-rich intermediate water was redistributed to the wide range of water density (shallower than  $26.6 \sigma_\theta$ ) via strong diapycnal tidal mixing at the Kuril strait [*Ono et al.*, 2007; *Itoh et al.*, 2010], and the mixed water was subsequently transported to the Oyashio region (data not shown). Thus, the Fe-rich intermediate water influences over a broad depth range along A line (Figure 7), and the depth of winter mixing enabled to reach the diss-Fe rich water shallower than  $26.6 \sigma_\theta$  before MLD reach to maximum depth (Figure 7). Therefore, existence of the lateral transport of Fe-rich intermediate water and the upward transport of materials from the intermediate water to the surface via the tidal mixing at Kuril strait [*Ono et al.*, 2007; *Itoh et al.*, 2010] and winter deep vertical water mixing [*Talley*, 1991; *Suga et al.*, 2004; X. Nakamura et al., manuscript in preparation, 2011], are important mechanisms to explain the high diss-Fe concentrations in the surface layer.

[30] The residence time of Fe in the intermediate water is still unknown. The time scale of the intermediate water transport from northwestern continental shelf to southern part in the Sea of Okhotsk (the Kuril basin) is less than half a year [*Ohshima et al.*, 2002]. The residence time of the OSIW in the Kuril basin has been estimated in the range from 1 to 10 years by several studies [*Yamamoto et al.*, 2002; *Itoh et al.*, 2003; *Gladyshev et al.*, 2003]. Therefore, the order of residence time of Fe in the intermediate layer is likely to be longer than surface mixed layer (month to year), and the longer residence time is necessary to explain the long distance transport of sedimentary Fe into the study region. Similar long distance sedimentary Fe transports were reported in other regions [e.g., *Bowie et al.*, 2009; *Slemons et al.*, 2010]. Numerical modeling of the Fe distributions in

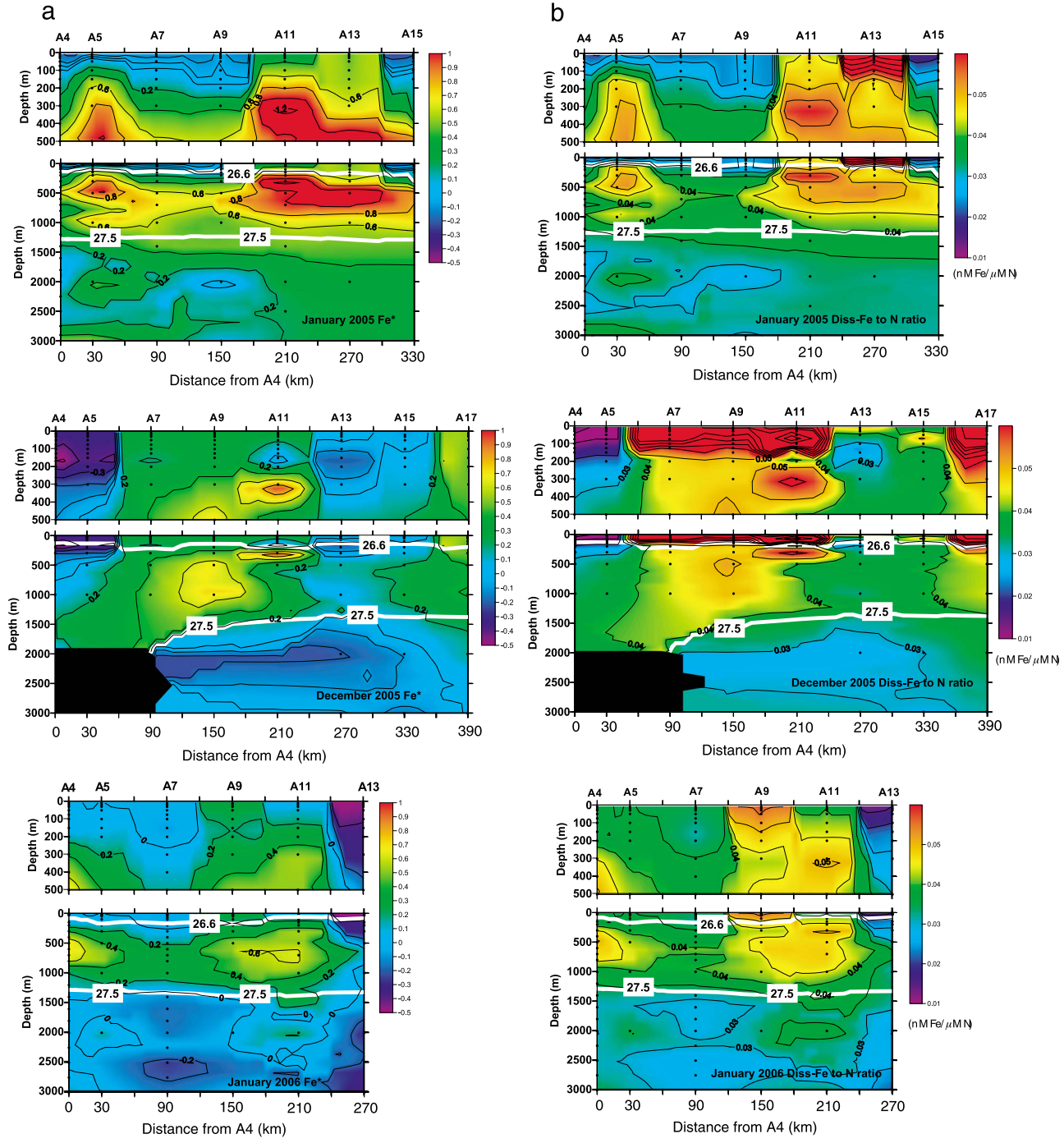


**Figure 9.** Vertical section profiles of (a)  $\text{Fe}^*$  and (b) diss-Fe to nitrate ratio ( $\text{nM diss-Fe} / (\mu\text{M NO}_3)^{-1}$ ) along the A line in the January 2005, December 2005, and January 2006.

the North Pacific indicated that a longer residence time for diss-Fe in the intermediate layer is necessary in order to match the observed concentrations, and Fe speciation is important factor to control the residence time (Misumi et al., submitted). We require a better understanding of residence time of Fe in the intermediate water, and the conversion of Fe between dissolved and particulate phase during the transport of intermediate waters.

[31] The winter diss-Fe supply process via the intermediate water transport and winter mixing can explain the significant and regular occurrence of the phytoplankton bloom in the Oyashio and Oyashio-Kuroshio transition zone during spring, because the turbulent winter mixing process can increase the surface Fe concentration every winter in time for the spring phytoplankton bloom, and such a consistent pattern is unlikely to occur based on the sporadic Fe supply from the airborne dust events.

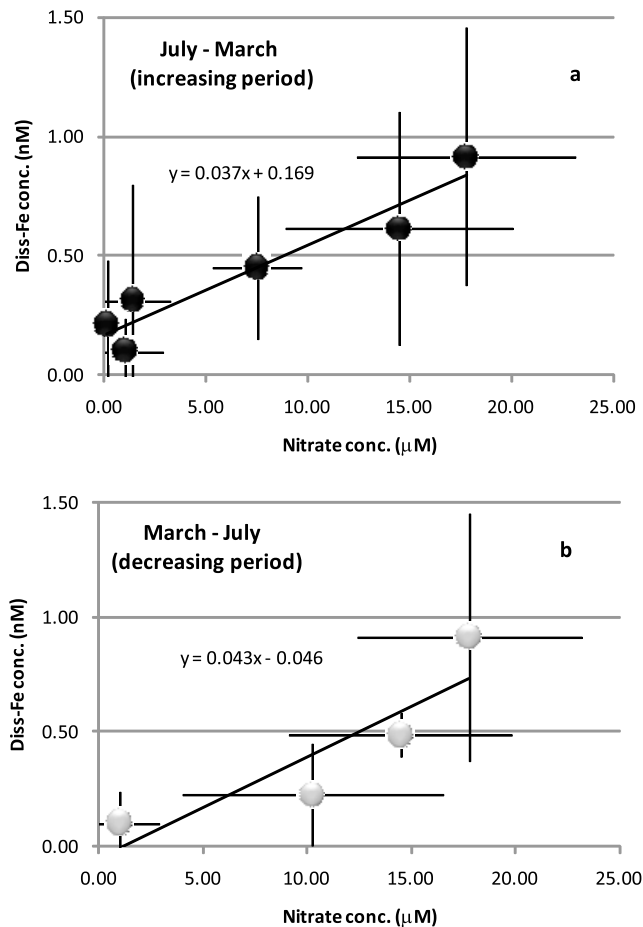


**Figure 10.** Diss-Fe versus nitrate plot from monthly compiled surface concentration along the A line in the Oyashio region. (a) Decreasing period in Figure 4 and (b) increasing period in Figure 4. Data are same as those of Figure 4.

#### 4.4. Quantitative Estimation of Diss-Fe Flux From the Subsurface Layer to the Surface

[32] We can estimate the annual upward diss-Fe flux, which is a revised value of *Nishioka et al.* [2007], using the seasonal diss-Fe data set obtained in this study. Diss-Fe profiles at Station A11 in January 2005 (Figure 8) and mean value of monthly compiled surface value (Figure 4) are used for this estimation. Total annual upward diss-Fe flux =  $F_1$  (Ekman advection and eddy diffusion flux) +  $F_2$  (winter mixing flux) ( $\mu\text{mol m}^{-2} \text{yr}^{-1}$ ).

$$F_1 = W \times R \times 215_{\text{days}} + Kz \times (dFe = dz) \times 215_{\text{days}},$$

$$F_2 = (C_1 - C_2) \times D_1.$$

[33] For  $F_1$ , where  $W$  is the vertical velocity with a value of  $0.012 \text{ m d}^{-1}$  [Martin *et al.*, 1989],  $R$  is the mean concentration of diss-Fe in the vertical gradient in the subsurface layer ( $1.2 \text{ nM}$ ). Global mean  $5 \text{ m}^2 \text{ d}^{-1}$  for the coefficient of eddy diffusivity ( $Kz$ ) and calculated  $dFe/dz$  gradient in dissolved Fe with depth ( $0.0085 \mu\text{mol m}^{-4}$ ) from our data set was employed. We use a simple straight forward method to estimate the winter upward flux caused by winter

mixing ( $F_2$ ). We define the winter period as 5 months (150 days) for this estimation, therefore, the formula of vertical advection and eddy diffusion in  $F_1$  is used as an estimation for the remaining 215 days. The winter maximum diss-Fe concentration in the MLD ( $0.92 \text{ nM}$ : mean value in March from Figure 4) was used for  $C_1$  instead of the summer dissolved Fe concentration at the maximum depth of the winter mixed layer of *Nishioka et al.* [2007], and  $C_2$  is diss-Fe concentration in the summer surface mixed layer ( $0.1 \text{ nM}$ : mean value in July from Figure 4), respectively.  $D_1$  is the summer surface mixed layer depth (20 m). The tidal mixing at Kuril strait can be omitted in this calculation, because we use the Fe profile in the Oyashio region in the calculations, which reflect results of redistribution of Fe by the tidal mixing processes. The estimated annual upward diss-Fe fluxes by Ekman advection and eddy diffusion flux are  $3.1$  and  $9.1 \mu\text{mol Fe m}^{-2} \text{ yr}^{-1}$ , respectively. The estimated annual upward flux by the winter mixing processes is  $16.4 \mu\text{mol Fe m}^{-2} \text{ yr}^{-1}$ , which comprises 57% of the total annual upward flux ( $28.6 \mu\text{mol Fe m}^{-2} \text{ yr}^{-1}$ ) in this region. Surface residence time of diss-Fe has been reported over a wide range of the tropical and subtropical Atlantic Ocean to range from 1.5 to 5 months [Bergquist and Boyle, 2006]. If we consider the surface residence time of diss-Fe is shorter than 150 day (winter period of our estimate), our estimate for the upward diss-Fe flux is underestimated. Estimates of atmospheric dust deposition reported by *Fung et al.* [2000], results of the ocean global model including Fe, suggest that the total atmospheric dust flux in the western North Pacific is  $929 \mu\text{mol Fe m}^{-2} \text{ yr}^{-1}$  (average value for  $40^\circ\text{N}, 170^\circ\text{E}$ ). Another reported rate of annual dust deposition in the WSP is  $0.3 \text{ g m}^{-2} \text{ yr}^{-1}$  [Measures *et al.*, 2005] or  $267 \mu\text{mol Fe m}^{-2} \text{ yr}^{-1}$  for a 5% Fe content. Recent reported solubility of airborne Fe in the WSP ranged from 1.2% to 2.2% (the bulk aerosol sample value [*Ooki et al.*, 2009]). If we employ these dust Fe information, the total upward iron flux ( $28.6 \mu\text{mol Fe m}^{-2} \text{ yr}^{-1}$ ) from intermediate waters to the surface in the Oyashio region would be larger than the atmospheric dust flux ( $3.2\text{--}20.4 \mu\text{mol Fe m}^{-2} \text{ yr}^{-1}$ ). These simple calculations suggest that the upward diss-Fe flux is particularly significant in the Oyashio region in the winter season, and probably higher than the atmospheric Fe input. Although the simple estimation suggests the upward flux would be larger than the atmospheric dust flux, the quantitative estimation based on previous information on dust deposition to this region indicated that the dust Fe supply cannot be dismissed for biological production. Probably, the airborne dust Fe input is more sporadic, and the spatial scale is larger than oceanic water mass scale, and therefore the impact would be spatiotemporally limited, and it may have a role in sporadically inducing phytoplankton blooms in the open ocean rather than as the principle source of Fe to initiate consistently occurring events such as the spring phytoplankton bloom in the Oyashio and the Oyashio-Kuroshio transition zone.

#### 4.5. Potential to Stimulate Phytoplankton Growth

[34] Mindful of observed diss-Fe and nitrate concentration in the surface and the intermediate water distributed heterogeneously in this area (Figure 7), we compared the diss-Fe to nitrate ( $\text{nM diss-Fe} / (\mu\text{M NO}_3)^{-1}$ ) ratio between the winter surface water and the intermediate water to begin with this

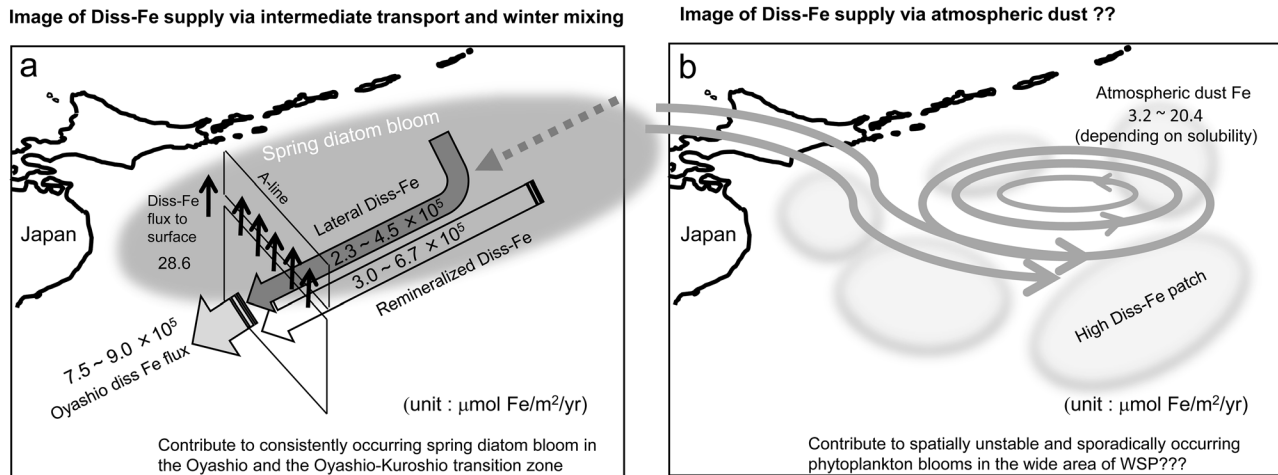


**Figure 11.** Schematic image of Fe supply processes in the WSP. (a) Diss-Fe supply via intermediate transport and winter mixing in the WSP which is described in this study. (b) Diss-Fe supply via atmospheric dust in the WSP. High mineral dust concentrations are transported by the movement of a low-pressure system over Japan. Values are estimated in sections 4.3 and 4.4.

discussion. The section profile of diss-Fe to nitrate ratio (Figure 9b) indicates that the Fe-rich intermediate water has a higher diss-Fe/NO<sub>3</sub> ratio ( $0.040 \pm 0.014$ , mean  $\pm$  1SD) than the surrounding water mass. The higher diss-Fe/NO<sub>3</sub> ratio in the intermediate water also suggests decoupling of diss-Fe from the nitrate cycle as described above for phosphate (in section 4.3). A substantially high diss-Fe/NO<sub>3</sub> ratio of  $0.036 \pm 0.028$  (mean  $\pm$  1SD) in the winter surface layer was calculated from all the data from the vertical sections (January 2005, December 2005, January 2006) and underway survey (January 2008), and this ratio value falls in the range which can be explained by the subsurface water influence. The mean value of the surface  $\Delta(\text{diss-Fe})/\Delta(\text{NO}_3)$  ratio during the diss-Fe increasing period from summer to winter (0.037), which was calculated by the slope of the surface diss-Fe versus NO<sub>3</sub> plot of monthly compiled data (Figure 4) in this period along the A line (Figure 10a), is also consistent with the diss-Fe/NO<sub>3</sub> ratio in the intermediate water. These results indicate that the winter surface water diss-Fe/NO<sub>3</sub> ratio was influenced by the Fe-rich intermediate water. The substantially higher diss-Fe/NO<sub>3</sub> ratio in the winter surface layer in this studied area than other HNLC region (as  $\sim 0.010$  in ESP [Nishioka et al., 2007] and  $0.010 - 0.025$  in the Southern Ocean [Ellwood et al., 2008]) indicates that the winter surface water in the Oyashio and the Oyashio-Kuroshio transition zone has a high potential to stimulate phytoplankton growth caused by the high Fe availability allowing high potential of macronutrients utilization. Harrison et al. [2004] compared the variability in biogeochemical processes and ecosystem structure in the WSP and the ESP based on observations from two time series stations [Tsurushima et al., 2002; Imai et al., 2002; Whitney and Freeland, 1999; Wong et al., 2002] and indicated that the winter surface mixing with nutrient rich subsurface waters in the Oyashio region and western subarctic gyre would lead to greater addition of nutrients to the surface water, and drive a larger seasonal amplitude in chlorophyll *a* and primary productivity in the WSP than in the ESP. Interpretation of

our data is consistent with these previous studies, and diss-Fe supply process via the intermediate water can be the leading cause for the longitudinal differences in biological production between the WSP and the ESP.

#### 4.6. Iron Limitation for Spring Diatom Bloom

[35] Details of spring biological production in the Oyashio and the Oyashio-Kuroshio transition zone has been extensively investigated and reported. A diatom bloom consistently occurs each spring [Saito et al., 2002; Okamoto et al., 2010], and the diatom bloom is terminated without major nutrient depletion [Saito et al., 2002]. A shift in the flora occurs after the diatom bloom with dinoflagellates increasing and consuming the major nutrients when the phytoplankton standing stock is low during summer [Mochizuki et al., 2002]. In order to understand the limiting nutrient for the spring diatom bloom in this region, the diss-Fe/NO<sub>3</sub> ratio is a useful index. According to the reported small Fe quota for oceanic diatoms,  $2 - 5 \mu\text{mol Fe} (\text{mol C})^{-1}$  [Sunda and Huntsman, 1995; Maldonado and Price, 1996; Marchetti and Harrison, 2007], and Redfield ratio, the minimum phytoplankton utilizing diss-Fe/NO<sub>3</sub> ratio calculated from the small Fe quota was range in  $0.013 - 0.033$  (nM diss-Fe ( $\mu\text{M NO}_3$ )<sup>-1</sup>). The dominant phytoplankton in the spring bloom in the Oyashio and the Oyashio-Kuroshio transition zone are large centric diatoms [Mochizuki et al., 2002; Tsuda et al., 2005]. Although the reported utilization diss-Fe/NO<sub>3</sub> ratios for diatoms are variable, the large centric diatoms probably have a higher diss-Fe/NO<sub>3</sub> uptake ratio than this minimum value, because large oceanic diatoms have higher cellular Fe quotas [Timmermans et al., 2001]. Additionally, luxury uptake at high Fe concentrations was observed in culture experiments of oceanic and coastal eukaryotic algae, and cellular Fe quotas can be greater in several orders than when they are Fe limited [Sunda and Huntsman, 1995, 1997; Sunda, 2001; Iwade et al., 2006; Yoshida et al., 2006]. On the other hand, mean value of  $\Delta(\text{diss-Fe})/\Delta(\text{NO}_3)$  consumption ratio during the diss-Fe

decreasing period from winter to summer, which was calculated from the slope of the surface diss-Fe versus  $\text{NO}_3^-$  plot of monthly compiled data (Figure 4) in this period along the A line, is 0.043 (Figure 10b). These results indicate that the phytoplankton utilizing (include transformation loss from the diss-Fe fraction) the diss-Fe/ $\text{NO}_3^-$  ratio are probably comparable to or slightly higher than supplied diss-Fe/ $\text{NO}_3^-$  ratio in the winter surface mixed layer, except for some water masses such as the coastal Oyashio area (low-salinity water less than 33, Figure 5). Therefore, from the aspect of mean value of diss-Fe/ $\text{NO}_3^-$  ratio, both diss-Fe and nitrate would be limiting nutrients for the spring diatom bloom. As described in section 3.1, the diss-Fe was depleted in some water masses in May, prior to nitrate depletion (Figure 4 and Table S1). These results indicate that in a substantial area of the Oyashio and the Oyashio-Kuroshio transition zone, diss-Fe in the winter surface was insufficient for diatoms to deplete the nitrate concentration at the termination of the diatom bloom. This interpretation is supported by other studies. *Saito et al.* [2002] showed an increase in silicate to nitrate uptake ratio at the end of the phytoplankton bloom in the Oyashio region. They suggested the increase in the silicate to nitrate ratio was due to light or Fe limitation as indicated by *Takeda* [1998]. *Hattori-Saito et al.* [2010] also reported that bloom-forming diatoms  $>20 \mu\text{m}$  were stressed by Fe availability in the Oyashio and the Oyashio-Kuroshio transition zone during spring, which was indicated by immunological ferredoxin/flavodoxin assay analysis. Furthermore, the multidecadal decrease in the spring net community production has been observed in the Oyashio region in the recent 30 years in conjunction with a long-term trend of surface stratification, despite that macronutrients in the mixed layer remained at the termination stage of the spring diatom bloom [*Ono et al.*, 2002; *Chiba et al.*, 2004; *Tadokoro et al.*, 2005]. This phenomenon can be explained if we assume that the Fe is the limiting nutrient for the spring Oyashio community, and the Fe fueling the seasonal diatom bloom is mainly supplied by the winter entrainment rather than by airborne dust events.

## 5. Conclusion

[36] Temporal variability of the diss-Fe concentration in the Oyashio and the Oyashio-Kuroshio transition zone was investigated using observations over a 5 year time series. The annual cycle of the diss-Fe concentration in the surface water occurred every year. Dissolved Fe supplied every winter into the surface water, and the diss-Fe concentration was drawn down during the spring bloom period probably due to rapid transformation and biological uptake. Then, diss-Fe is depleted in summer in some water masses in this region and increases from autumn to winter with the increase of the surface mixed layer depth. The high diss-Fe concentration in the winter surface layer was controlled by mesoscale oceanic processes, and differences in the magnitude of winter mixing processes among each water mass caused the heterogeneous spatial distribution of diss-Fe in the surface layer. Vertical section profiles along the observed line suggested the occurrence of Fe-rich intermediate water beneath the surface, and the intermediate water is also important to explain the high diss-Fe concentrations in the surface layer in winter. From analysis of the observed

and reported phytoplankton utilizing diss-Fe/ $\text{NO}_3^-$  ratio, we conclude that the winter surface water has a high potential to stimulate phytoplankton growth with macronutrients utilization. However, the diss-Fe supplied in the winter surface layer was insufficient to consume all the nitrate in the water with the growth of diatom, although in some part of the region was clearly depleted in nitrate prior to diss-Fe. Airborne dust Fe supply is an undeniable Fe source for open ocean phytoplankton growth. However, the scale and timing of the dust inputs is inadequate to explain it as the major driving phenomenon of the annual Fe cycle. Probably, the airborne dust Fe input is more sporadic, and the spatial scale is larger than oceanic water mass scale, and therefore the impact would be spatiotemporally limited, and it may have a role for sporadically occurring phytoplankton blooms in the open ocean rather than the consistently occurring events such as the spring phytoplankton bloom in the Oyashio and the Oyashio-Kuroshio transition zone. Our study implies that a different source of Fe fuels different phenomenon of biological production in this region (Figure 11). The result of this study is compatible to *Nishioka et al.* [2007], which indicates that the lateral transport of Fe from a marginal sea and continental margin as well as vertical mixing are key processes to explain the high biological response in the WSP.

[37] **Acknowledgments.** We express our appreciation and thanks to the crew and officers of R/V *Hokko-Maru*, *Tankai-Maru*, *Oshoro-Maru*, and *Wakataka-Maru*, for their assistance. Thanks are also extended to A. Murayama for her assistance with the laboratory work. We thank P. W. Boyd, T. Nakatsuka, T. Shiraiwa, S. Matoba, Y. W. Watanabe, and anonymous reviewers for their helpful comments. This work was supported by the Ministry of Education, Science and Culture 20221002 and by the Grant-in-Aid for Scientific Research in Priority Areas “Western Pacific Air-Sea Interaction Study (W-PASS)” under grants 19030002, 21014001, and also the Basic Research Grant “Study for iron dynamics and ecosystem response in the Oyashio region” under grant 16310039, by the Agriculture, Forestry and Fisheries Research Council project fund “Evaluation, Adaptation and Mitigation of Global Warming in Agriculture, Forestry and Fisheries: Research and Development,” and by the Central Research Institute of Electric Power Industry. Part of this work is supported by the Amur-Okhotsk Project, promoted by the Research Institute for Humanity and Nature (RIHN).

## References

- Anderson, L., and J. Sarmiento (1994), Redfield ratios of remineralization determined by nutrient data analysis, *Global Biogeochem. Cycles*, 8, 65–80, doi:10.1029/93GB03318.
- Bergquist, B. A., and E. A. Boyle (2006), Dissolved iron in the tropical and subtropical Atlantic Ocean, *Global Biogeochem. Cycles*, 20, GB1015, doi:10.1029/2005GB002505.
- Blain, S., G. Sarthou, and P. Laan (2008), Distribution of dissolved iron during the natural iron fertilization experiment KOEPS (Kerguelen Plateau, Southern Ocean), *Deep Sea Res., Part II*, 55, 594–605, doi:10.1016/j.dsr2.2007.12.028.
- Bowie, A. R., D. Lannuzel, T. A. Remenyi, T. Wagener, P. J. Lam, P. W. Boyd, C. Guieu, A. T. Townsend, and T. W. Trull (2009), Biogeochemical iron budgets of the Southern Ocean south of Australia: Decoupling of iron and nutrient cycles in the subantarctic zone by the summertime supply, *Global Biogeochem. Cycles*, 23, GB4034, doi:10.1029/2009GB003500.
- Boyd, P. W., et al. (2004), The decline and fate of an iron-induced subarctic phytoplankton bloom, *Nature*, 428, 549–553, doi:10.1038/nature02437.
- Boyd, P. W., M. P. Gall, M. W. Silver, S. L. Coale, R. R. Bidigare, and J. L. K. B. Bishop (2008), Quantifying the surface-subsurface biogeochemical coupling during the VERTIGO ALOHA and K2 studies, *Deep Sea Res., Part II*, 55, 1578–1593, doi:10.1016/j.dsr2.2008.04.010.
- Boyle, E. A., B. A. Bergquist, R. A. Kayser, and N. Mahowald (2005), Iron, manganese, and lead at Hawaii ocean time-series station ALOHA: Temporal variability and an intermediate water hydrothermal plume,

- Geochim. Cosmochim. Acta*, 69(4), 933–952, doi:10.1016/j.gca.2004.07.034.
- Buck, C. S., W. M. Landing, J. A. Resing, and G. T. Lebon (2006), Aerosol iron and aluminum solubility in the northwest Pacific Ocean: Results from the 2002 IOC cruise, *Geochim. Geophys. Geosyst.*, 7, Q04M07, doi:10.1029/2005GC000977.
- Buesseler, K. O., et al. (2007), Revisiting carbon flux through the ocean's twilight zone, *Science*, 316, 567–570, doi:10.1126/science.1137959.
- Chase, Z., B. Hales, and T. Cowles (2005), Distribution and variability of iron input to Oregon coastal waters during the upwelling season, *J. Geophys. Res.*, 110, C10S12, doi:10.1029/2004JC002590.
- Chiba, S., T. Ono, K. Tadokoro, T. Midorikawa, and T. Saino (2004), Increased stratification and decreased lower trophic level productivity in the Oyashio region of the North Pacific: A 30-year retrospective study, *J. Oceanogr.*, 60, 149–162, doi:10.1023/B:JOCE.0000038324.14054.cf.
- Chierici, M., A. Fransson, and Y. Nojiri (2006), Biogeochemical processes as drivers of surface fCO<sub>2</sub> in contrasting provinces in the subarctic North Pacific Ocean, *Global Biogeochem. Cycles*, 20, GB1009, doi:10.1029/2004GB002356.
- Croot, P. L., and K. A. Hunter (1998), Trace metal distributions across the continental shelf near Otago Peninsula, New Zealand, *Mar. Chem.*, 62, 185–201, doi:10.1016/S0304-4203(98)00036-X.
- Croot, P. L., K. Andersson, M. Öztürk, and D. R. Turner (2004), The distribution and speciation of iron along 6°E in the Southern Ocean, *Deep Sea Res., Part II*, 51, 2857–2879, doi:10.1016/j.dsrr.2003.10.012.
- Cullen, J. T., M. Chong, and D. Ianson (2009), British Columbian continental shelf as a source of dissolved iron to the subarctic northeast Pacific Ocean, *Global Biogeochem. Cycles*, 23, GB4012, doi:10.1029/2008GB003326.
- Duce, R. A., and N. W. Tindale (1991), Atmospheric transport of iron and its deposition in the ocean, *Limnol. Oceanogr.*, 36, 1715–1726, doi:10.4319/lo.1991.36.8.1715.
- Dulaiova, H., M. V. Ardelan, P. B. Henderson, and M. A. Charette (2009), Shelf-derived iron inputs drive biological productivity in the southern Drake Passage, *Global Biogeochem. Cycles*, 23, GB4014, doi:10.1029/2008GB003406.
- Ellwood, M. J., P. W. Boyd, and P. Sutton (2008), Winter-time dissolved iron and nutrient distributions in the Subantarctic Zone from 40–52°S; 155–160°E, *Geophys. Res. Lett.*, 35, L11604, doi:10.1029/2008GL033699.
- Elrod, V. A., W. M. Berelson, K. H. Coale, and K. S. Johnson (2004), The flux of iron from continental shelf sediment: A missing source for global budget, *Geophys. Res. Lett.*, 31, L12307, doi:10.1029/2004GL020216.
- Elrod, V. A., K. S. Johnson, S. E. Fitzwater, and J. N. Plant (2008), A long-term, high-resolution record of surface water iron concentrations in the upwelling-driven central California region, *J. Geophys. Res.*, 113, C11021, doi:10.1029/2007JC004610.
- Fung, I. Y., S. K. Meyn, I. Tegen, S. C. Doney, J. G. John, and J. K. Bishop (2000), Iron supply and demand in the upper ocean, *Global Biogeochem. Cycles*, 14, 281–295, doi:10.1029/1999GB900059.
- Gladyshev, S., L. Talley, G. Khen, and M. Wakatsuchi (2003), Distribution, formation, and seasonal variability of Okhotsk Sea mode water, *J. Geophys. Res.*, 108(C6), 3186, doi:10.1029/2001JC000877.
- Harrison, P. J., F. A. Whitney, A. Tsuda, H. Saito, and K. Tadokoro (2004), Nutrient and phytoplankton dynamics in the NE and NW gyres of the subarctic Pacific Ocean, *J. Oceanogr.*, 60, 93–117, doi:10.1023/B:JOCE.0000038321.57391.2a.
- Hattori-Saito, A., J. Nishioka, T. Ono, R. M. L. McKay, and K. Suzuki (2010), Fe deficiency in micro-sized diatoms in the Oyashio region of the western subarctic Pacific during spring, *J. Oceanogr.*, 66, 105–115, doi:10.1007/s10872-010-0009-9.
- Honda, M. C. (2003), Biological pump in the northwestern North Pacific, *J. Oceanogr.*, 59, 671–684, doi:10.1023/B:JOCE.0000009596.57705.0c.
- Imai, K., Y. Nojiri, N. Tsurushima, and T. Saino (2002), Time series station of seasonal variation of primary production at station KNOT (44°N, 155°E) in the subarctic western North Pacific, *Deep Sea Res., Part II*, 49, 5395–5408, doi:10.1016/S0967-0645(02)00198-4.
- Itoh, M., K. I. Ohshima, and M. Wakatsuchi (2003), Distribution and formation of Okhotsk Sea intermediate water: An analysis of isopycnal climatological data, *J. Geophys. Res.*, 108(C8), 3258, doi:10.1029/2002JC001590.
- Itoh, S., I. Yasuda, T. Nakatsuka, J. Nishioka, and Y. N. Volkov (2010), Fine- and microstructure observations in the Urum Strait, Kuril Island, during August 2006, *J. Geophys. Res.*, 115, C08004, doi:10.1029/2009JC005629.
- Iwade, S., K. Kuma, Y. Isoda, M. Yoshida, I. Kudo, J. Nishioka, and K. Suzuki (2006), Effect of iron concentrations on iron uptake and growth of a coastal diatom *Chaetoceros sociale*, *Aquat. Microb. Ecol.*, 43, 177–191, doi:10.3354/ame043177.
- Jickells, T. D., and L. J. Spokes (2001), Atmospheric iron inputs to the oceans, in *The Biogeochemistry of Iron in Seawater*, pp. 85–121, John Wiley, New York.
- Johnson, K. S., F. P. Chavez, and G. E. Friederich (1999), Continental-shelf sediment as a primary source of iron for coastal phytoplankton, *Nature*, 398, 697–700, doi:10.1038/19511.
- Johnson, K. S., F. P. Chavez, V. A. Elrod, S. E. Fitzwater, J. T. Pennington, K. R. Buck, and P. M. Walz (2001), The annual cycle of iron and the biological response in central California coastal waters, *Geophys. Res. Lett.*, 28, 1247–1250, doi:10.1029/2000GL012433.
- Johnson, K. S., et al. (2003), Surface ocean-lower atmosphere interaction in the North Pacific Ocean gyre: Aerosols, iron, and the ecosystem response, *Global Biogeochem. Cycles*, 17(2), 1063, doi:10.1029/2002GB002004.
- Johnson, K. S., et al. (2007), Developing standards for dissolved iron in seawater, *Eos Trans. AGU*, 88(11), 131–132, doi:10.1029/2007EO110003.
- Johnson, W. K., L. A. Miller, N. E. Sutherland, and C. S. Wong (2005), Iron transport by mesoscale Haida eddies in the Gulf of Alaska, *Deep Sea Res., Part II*, 52, 933–953, doi:10.1016/j.dsrr.2004.08.017.
- Lam, P. J., and J. K. B. Bishop (2008), The continental margin is a key source of iron to the HNLC North Pacific Ocean, *Geophys. Res. Lett.*, 35, L07608, doi:10.1029/2008GL033294.
- Lam, P. J., J. K. B. Bishop, C. C. Henning, M. A. Marcus, G. A. Waychunas, and I. Y. Fung (2006), Wintertime phytoplankton bloom in the subarctic Pacific supported by continental margin iron, *Global Biogeochem. Cycles*, 20, GB1006, doi:10.1029/2005GB002557.
- Levitus, S. (1982), Climatological Atlas of the World Ocean, *NOAA Prof. Pap.*, 13, 191 pp.
- Longhurst, A., S. Sathyendranath, T. Platt, and C. Caverhill (1995), An estimate of global primary production in the ocean from satellite radiometer data, *J. Plankton Res.*, 17, 1245–1271, doi:10.1093/plankt/17.6.1245.
- Mahowald, N. M., A. R. Baker, G. Bergametti, N. Brooks, A. Duce, T. D. Jickells, N. Kubilay, J. M. Prospero, and I. Tegen (2005), Atmospheric global dust cycle and iron inputs to the ocean, *Global Biogeochem. Cycles*, 19, GB4025, doi:10.1029/2004GB002402.
- Maldonado, M. T., and N. M. Price (1996), Influence of N substrate on Fe requirements of marine centric diatom, *Mar. Ecol. Prog. Res.*, 141, 161–172, doi:10.3354/meps141161.
- Marchetti, A., and P. J. Harrison (2007), Coupled changes in the cell morphology and the elemental (C, N, and Si) composition of the pennate diatom pseudo-nitzschia due to iron deficiency, *Limnol. Oceanogr.*, 52(5), 2270–2284, doi:10.4319/lo.2007.52.5.2270.
- Martin, J. H., R. M. Gordon, S. Fitzwater, and W. W. Broenkow (1989), VERTEX: Phytoplankton/iron studies in the Gulf of Alaska, *Deep Sea Res., Part I*, 36(5), 649–680, doi:10.1016/0198-0149(89)90144-1.
- Measures, C. I., M. T. Brown, and S. Vink (2005), Dust deposition to the surface waters of the western and central North Pacific inferred from surface water dissolved aluminium concentrations, *Geochim. Geophys. Geosyst.*, 6, Q09M03, doi:10.1029/2005GC000922.
- Mochizuki, M., N. Shiga, M. Saito, K. Imai, and Y. Nojiri (2002), Seasonal change in nutrients, chlorophyll-a, phytoplankton assemblage of the western subarctic gyre in the Pacific Ocean, *Deep Sea Res., Part II*, 49, 5421–5439, doi:10.1016/S0967-0645(02)00209-6.
- Moore, J. K., and O. Braucher (2008), Sedimentary and mineral dust sources of dissolved iron to the world ocean, *Biogeosciences*, 5, 631–656, doi:10.5194/bg-5-631-2008.
- Nishioka, J., S. Takeda, C. S. Wong, and W. K. Johnson (2001), Size-fractionated iron concentrations in the northeast Pacific Ocean: Distribution of soluble and small colloidal iron, *Mar. Chem.*, 74, 157–179, doi:10.1016/S0304-4203(01)00013-5.
- Nishioka, J., S. Takeda, I. Kudo, D. Tsumune, T. Yoshimura, K. Kuma, and A. Tsuda (2003), Size-fractionated iron distributions and iron-limitation processes in the subarctic NW Pacific, *Geophys. Res. Lett.*, 30(14), 1730, doi:10.1029/2002GL016853.
- Nishioka, J., et al. (2007), Iron supply to the western subarctic Pacific: Importance of iron export from the Sea of Okhotsk, *J. Geophys. Res.*, 112, C10012, doi:10.1029/2006JC004055.
- Obata, H., H. Karatani, and E. Nakayama (1993), Automated determination of iron in seawater by chelating resin concentration and chemiluminescence detection, *Anal. Chem.*, 65, 1524–1528, doi:10.1021/ac00059a007.
- Obata, H., H. Karatani, M. Matsui, and E. Nakayama (1997), Fundamental studies for chemical speciation of iron in seawater with an improved analytical method, *Mar. Chem.*, 56, 97–106, doi:10.1016/S0304-4203(96)00082-5.
- Ohshima, K. I., M. Wakatsuchi, Y. Fukamachi, and G. Mizuta (2002), Near-surface circulation and tidal currents of the Okhotsk Sea observed with satellite-tracked drifters, *J. Geophys. Res.*, 107(C11), 3195, doi:10.1029/2001JC001005.

- Ohshima, K. I., T. Nakanowatari, S. Riser, and M. Wakatsuchi (2010), Seasonal variation in the in- and outflow of the Okhotsk Sea with the North Pacific, *Deep Sea Res., Part II*, 57, 1247–1256, doi:10.1016/j.dsr2.2009.12.012.
- Ohtani, K. (1989), The role of the Sea of Okhotsk on the formation of the Oyashio water (in Japanese with English abstract), *Umi Sora*, 65, 63–82.
- Okamoto, S., T. Hirawake, and S. Saito (2010), Interannual variability in the magnitude and timing of spring bloom in the Oyashio region, *Deep Sea Res., Part II*, 57, 1608–1617, doi:10.1016/j.dsr2.2010.03.005.
- Ono, K., K. I. Ohshima, T. Kono, M. Ito, K. Katsumata, Y. N. Volkov, and M. Wakatsuchi (2007), Water mass exchange and diapycnal mixing at Bussol' strait revealed by water mass properties, *J. Oceanogr.*, 63, 281–291, doi:10.1007/s10872-007-0028-3.
- Ono, T., K. Tadokoro, T. Midorikawa, J. Nishioka, and T. Saino (2002), Multi-decadal decrease of net community production in the western subarctic North Pacific, *Geophys. Res. Lett.*, 29(8), 1186, doi:10.1029/2001GL014332.
- Ono, T., H. Kasai, T. Midorikawa, Y. Takatani, K. Saito, M. Ishii, Y. W. Watanabe, and K. Sasaki (2005), Seasonal and interannual variation of DIC in surface mixed layer in the Oyashio region: A climatological view, *J. Oceanogr.*, 61, 1075–1087, doi:10.1007/s10872-006-0023-0.
- Ooki, A., J. Nishioka, T. Ono, and S. Noriki (2009), Size dependence of iron solubility of Asian mineral dust particles, *J. Geophys. Res.*, 114, D03202, doi:10.1029/2008JD010804.
- Parekh, P., M. J. Follows, and E. A. Boyle (2005), Decoupling of iron and phosphate in the global ocean, *Global Biogeochem. Cycles*, 19, GB2020, doi:10.1029/2004GB002280.
- Planquette, H., et al. (2007), Dissolved iron in the vicinity of the Crozet Islands, Southern Ocean, *Deep Sea Res., Part II*, 54, 1999–2019, doi:10.1016/j.dsr2.2007.06.019.
- Saito, H., A. Tsuda, and H. Kasai (2002), Nutrient and plankton dynamics in the Oyashio region of the western subarctic Pacific Ocean, *Deep Sea Res., Part II*, 49, 5463–5486, doi:10.1016/S0967-0645(02)00204-7.
- Schlitzer, R. (2004), Export production in equatorial and North Pacific derived from dissolved oxygen, nutrient and carbon data, *J. Oceanogr.*, 60, 53–62, doi:10.1023/B:JOCE.0000038318.38916.e6.
- Shimizu, Y., I. Yasuda, K. Okuda, K. Hanawa, and S. Ito (2003), ADCP-referenced Kuroshio and Oyashio water transports for North Pacific Intermediate Water formation, *J. Phys. Oceanogr.*, 33, 220–233, doi:10.1175/1520-0485(2003)033<0220:ARKAOW>2.0.CO;2.
- Slemons, L. O., J. W. Marry, J. Resing, B. Paul, and P. Dutrieux (2010), Western Pacific coastal sources of iron, manganese and aluminum to the Equatorial Undercurrent, *Global Biogeochem. Cycles*, 24, GB3024, doi:10.1029/2009GB003693.
- Suga, T., K. Motoki, and Y. Aoki (2004), The North Pacific climatology of winter mixed layer and mode waters, *J. Phys. Oceanogr.*, 34, 3–22, doi:10.1175/1520-0485(2004)034<0003:TNPCow>2.0.CO;2.
- Sunda, W. G. (2001), Bioavailability and bioaccumulation of iron in the sea, in *The Biogeochemistry of Iron in Seawater*, pp. 41–84, John Wiley, New York.
- Sunda, W. G., and S. A. Huntsman (1995), Iron uptake and growth limitation in oceanic and coastal phytoplankton, *Mar. Chem.*, 50, 189–206, doi:10.1016/0304-4203(95)00035-P.
- Sunda, W. G., and S. A. Huntsman (1997), Interrelated influence of iron, light and cell size on marine phytoplankton growth, *Nature*, 390, 389–392, doi:10.1038/37093.
- Tadokoro, K., S. Chiba, T. Ono, T. Midorikawa, and T. Saino (2005), Interannual variation in Neocalanus copepod biomass in the Oyashio water of the western North Pacific, *Fish. Oceanogr.*, 14, 210–222, doi:10.1111/j.1365-2419.2005.00333.x.
- Takahashi, T., et al. (2002), Global sea-air CO<sub>2</sub> flux based on climatological surface ocean pCO<sub>2</sub>, and seasonal biological and temperature effects, *Deep Sea Res., Part II*, 49, 1601–1622, doi:10.1016/S0967-0645(02)00003-6.
- Takeda, S. (1998), Influence of iron availability on nutrient consumption ratio of diatoms in oceanic waters, *Nature*, 393, 774–777, doi:10.1038/31674.
- Talley, L. D. (1991), An Okhotsk Sea Water anomaly: Implications for ventilation in the North Pacific, *Deep Sea Res., Part I*, 38, S171–S190.
- Timmermans, K. R., L. J. A. Gerringa, H. J. W. de Baar, B. van der Wagt, M. J. W. Veldhuis, J. T. M. de Jong, P. L. Croot, and M. Boye (2001), Growth rates of large and small Southern Ocean diatoms in relation to availability of iron in natural seawater, *Limnol. Oceanogr.*, 46, 260–266, doi:10.4319/lo.2001.46.2.0260.
- Tsuda, A., et al. (2003), A mesoscale iron enrichment in the western subarctic Pacific induces large centric diatom bloom, *Science*, 300, 958–961, doi:10.1126/science.1082000.
- Tsuda, A., H. Kiyosawa, A. Kuwata, M. Mochizuki, N. Shiga, H. Saito, S. Chiba, K. Imai, J. Nishioka, and T. Ono (2005), Response of diatoms to iron-enrichment (SEEDS) in the western subarctic Pacific, temporal and spatial comparisons, *Prog. Oceanogr.*, 64, 189–205, doi:10.1016/j.pocean.2005.02.008.
- Tsumune, D., J. Nishioka, A. Shimamoto, S. Takeda, and A. Tsuda (2005), Physical behavior of the iron fertilized patch by SF<sub>6</sub> tracer release experiment, *Prog. Oceanogr.*, 64, 111–127, doi:10.1016/j.pocean.2005.02.018.
- Tsurushima, N., Y. Nojiri, K. Imai, and S. Watanabe (2002), Seasonal variations of carbon dioxide system and nutrients in the surface mixed layer at station KNOT (44°N, 155°E) in the subarctic western North Pacific, *Deep Sea Res., Part II*, 49, 5377–5394, doi:10.1016/S0967-0645(02)00197-2.
- Uematsu, M., R. A. Duce, J. M. Prospero, L. Q. Chen, J. T. Merrill, and R. L. McDonald (1983), Transport of mineral aerosol from Asia over the North Pacific Ocean, *J. Geophys. Res.*, 88, 5343–5352, doi:10.1029/JC088iC09p05343.
- Uematsu, M., A. Yoshikawa, H. Muraki, K. Arao, and I. Uno (2002), Transport of mineral and anthropogenic aerosols during a Kosa event over East Asia, *J. Geophys. Res.*, 107(D7), 4059, doi:10.1029/2001JD000333.
- Vink, S., and C. I. Measures (2001), The role of dust deposition in the determining surface water distributions of Al and Fe in the south west Atlantic, *Deep Sea Res., Part II*, 48, 2787–2809, doi:10.1016/S0967-0645(01)00018-2.
- Welschmeyer, N. A. (1994), Fluorometric analysis of chlorophyll a in the presence of chlorophyll b and pheophytins, *Limnol. Oceanogr.*, 39, 1985–1992, doi:10.4319/lo.1994.39.8.1985.
- Whitney, F. A., and H. J. Freeland (1999), Variability in upper-ocean water properties in the NE Pacific Ocean, *Deep Sea Res., Part II*, 46, 2351–2370, doi:10.1016/S0967-0645(99)00067-3.
- Wong, C. S., N. A. D. Waser, Y. Nojiri, F. A. Whitney, J. S. Page, and J. Zeng (2002), Seasonal cycles of nutrients and dissolved inorganic carbon at high and mid latitudes in the North Pacific Ocean during the Skaugan cruises: Determination of new production and nutrient uptake ratios, *Deep Sea Res., Part II*, 49, 5317–5338, doi:10.1016/S0967-0645(02)00193-5.
- Yamamoto, M., S. Watanabe, S. Tsunogai, and M. Wakatsuchi (2002), Effect of sea ice formation and diapycnal mixing on the Okhotsk Sea intermediate water clarified with oxygen isotopes, *Deep Sea Res., Part I*, 49, 1165–1174, doi:10.1016/S0967-0637(02)00032-8.
- Yasuda, I. (1997), The origin of the North Pacific Intermediate Water, *J. Geophys. Res.*, 102(C1), 893–909, doi:10.1029/96JC02938.
- Yasuda, I., Y. Hiroe, K. Komatsu, K. Kawasaki, T. M. Joyce, F. Bahr, and Y. Kawasaki (2001), Hydrographic structure and transport of the Oyashio south of Hokkaido and the formation of North Pacific Intermediate Water, *J. Geophys. Res.*, 106(C4), 6931–6942, doi:10.1029/1999JC000154.
- Yoshida, M., K. Kuma, S. Iwade, Y. Isoda, H. Takata, and M. Yamada (2006), Effect of aging time on the availability of freshly precipitated ferric hydroxide to coastal marine diatoms, *Mar. Biol.*, 149, 379–392, doi:10.1007/s00227-005-0187-y.

J. Nishioka, Pan-Okhotsk Research Center, Institute of Low Temperature Science, Hokkaido University, Sapporo, Hokkaido 060-0819, Japan. (nishioka@lowtem.hokudai.ac.jp)

T. Ono, Hokkaido National Fisheries Research Institute, Kushiro, Hokkaido 085-0802, Japan.

H. Saito, Touhoku National Fisheries Research Institute, Shiogama, Miyagi 985-0001, Japan.

K. Sakaoka, Faculty of Fisheries Science, Hokkaido University, Hakodate, Hokkaido 041-0861, Japan.

T. Yoshimura, Central Research Institute of Electric Power Industry, Abiko, Chiba 270-1194, Japan.